

Experimental Analysis of External Cylindrical Surfaces of Mild Steel Using Modified Turning Type Magnetorheological Finishing Tool

A Dissertation Submitted
In Partial Fulfillment of the Requirements
for the Degree of

Master of Engineering
in
Production Engineering

By

Gagandeep Singh



to the

**MECHANICAL ENGINEERING DEPARTMENT
THAPAR UNIVERSITY, PATIALA**

July, 2016

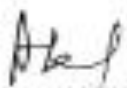
CERTIFICATE

I hereby declare that the thesis entitled "Experimental analysis of external cylindrical surfaces of mild steel using modified turning type magnetorheological finishing tool" is an authentic record of my study carried out as requirements for the award of the degree of **Master of Engineering in Production Engineering at Thapar University, Patiala** under the supervision of **Dr. Anant Kumar Singh**, Assistant Professor, Mechanical Engineering Department, Thapar University, Patiala during July, 2016. The matter embodied in this report has not been submitted in partial or full to any other university or institute for the award of any degree.

Date: 15/7/16


Gagandeep Singh

It is certified that the above statement made by the student is correct to the best of my/our knowledge and belief.


15/07/2016
Dr. Anant Kumar Singh
Assistant Professor
Mechanical Engineering Department
Thapar University, Patiala - 147004

Countersigned by


Dr. S. K. Mohapatra
Sr. Professor & Head
Mechanical Engineering Department
Thapar University, Patiala - 147004


Dr. S. S. Bhatia
Dean of Academic Affairs
Thapar University, Patiala - 147004

Dedicated
to
My Beloved Parents
who taught me
to
read and write

Acknowledgements

I am highly grateful to the authorities of Thapar University, Patiala for providing this opportunity to carry out the report work.

I would like to express a deep sense of gratitude and thank profusely to my thesis guides

Dr. Anant Kumar Singh for their sincere & invaluable guidance and suggestions which inspired me to submit thesis report in the present form.

I would also like to thank all the faculty and staff members of Mechanical engineering department for their intellectual support and unyielding encouragement.

Special thanks to Sahil Maan and Manpreet Singh for their support and advise regarding the thesis work.

Finally, I would like to extend my gratitude to all those persons who directly or indirectly helped me in the process and contributed towards this phase of my report work.

(Gagandeep Singh)

Abstract

The aim of this thesis is to design a new turning type MRF tool which had uniform magnetic field density at the tool tip. At first simulation for curve tip type turning type magnetorheological finishing tool has been performed in MAXWELL ANSOFT V13 student version to analysis the magnetic flux density distribution at the tool tip and compared with the existing tool having flat tip surface. From, the magnetic simulations clearly seen that the magnetic flux density on curve type tool tip surface is much more uniform than the existing flat tool tip surface at same parametric conditions. The new curve tip turning type magnetorheological finishing tool has been fabricated with same dimensions of existing flat tool and attached at the selected lathe machine.

To optimize the process performance of the present fabricated curve tip magnetorheological finishing tool, the design of experiments were carried out with major selected process parameters such as working gap, magnetizing current, workpiece rotating speed and abrasive mesh size. The experiments plan and analysis have been done by using DESIGN EXPERT- 10 software. The experimental responses were measured in terms of percentage change in R_a values. The experiments have been performed on each specimen at 60 minutes of finishing time. The best surface roughness value obtained on mild steel workpiece was 170 nm from the initial surface roughness value 680 nm at finishing condition as current 3.5A, working gap 1mm, workpiece rotational speed 300 rpm and abrasive 600 mesh size. It is found that the abrasive mesh size is most significant factor in affecting the percentage change in the roughness value of the mild steel workpiece. On the basis of experimental results, the optimum process parameters were predicted from the regression model for maximum percentage change in R_a value. The surface roughness reduction value on mild steel workpiece was 120 nm from the initial surface roughness value 720 nm at optimum finishing conditions as rotational speed of tool core 150 rpm, magnetizing current 3.5A, working gap 0.5 mm and abrasive 600 mesh size. The surface roughness was measured with Mitotoyo SJ-400 surface roughness tester. The scanning electron microscopy has been also used to know the final finished surface quality.

Contents

| | |
|---|------|
| List of figures | ix |
| List of tables | xii |
| Nomenclature | xiii |
| Acronyms | xiv |
| 1. Introduction | |
| 1.1 Introduction | 1 |
| 1.2 Conventional finishing process | 2 |
| 1.2.1 Grinding process | 2 |
| 1.2.2 Lapping process | 3 |
| 1.2.3 Honing process | 3 |
| 1.3 Advanced finishing processes | 3 |
| 1.3.1 Magnetorheological finishing | 3 |
| 1.3.2 Magnetic abrasive finishing | 5 |
| 1.3.3 Magnetorheological abrasive flow finishing | 6 |
| 1.3.4 Magnetic float polishing | 8 |
| 1.3.5 Magnetorheological jet finishing | 9 |
| 1.3.6 Ball end type magnetorheological finishing | 10 |
| 1.4 Advantage of Advanced Finishing processes | 11 |
| 1.5 Application of advanced finishing processes | 11 |
| 2. Literature review | |
| 2.1 Literature review | 12 |
| 2.2 Research gap | 22 |
| 2.3 Objective of the present work | 22 |
| 2.4 Methodology | 23 |
| 3. Magnetorheological finishing process for external cylindrical workpieces with turning type tool | |
| 3.1 Turning type magnetorheological process | 25 |
| 3.1.1 Mechanism of material removal | 26 |
| 3.2 Finite element analysis of the present turning type MRF tool | 27 |
| 3.3 Comparison Between MRF tool with flat tip surface and curve tip surface | 29 |

| | | |
|-----------|---|----|
| 3.3.1 | Comparison between MRF tool with flat tip surface and curve tip surface (experimentally) | 33 |
| 3.4 | Lathe machine specifications | 35 |
| 3.5 | CAD model of turning type MRF tool | 36 |
| 3.6 | Stirring machine to mixing the MRP fluid | 38 |
| 3.7 | Preliminary experiments on permanent mould punch die with curve tool tip surface of MRF turning type tool | 40 |
| 3.7.1 | Parameters and conditions | 41 |
| 3.7.2 | Result | 42 |
| 3.8 | Conclusion | 43 |
| 4. | Synthesis of MR polishing fluid and Experimentation | |
| 4.1 | Preparation of MRP fluid | 44 |
| 4.1.1 | Preparation of base fluid | 44 |
| 4.1.2 | MR polishing fluid | 45 |
| 4.2 | Turning type MRF process variables | 45 |
| 4.2.1 | Rotational speed of the workpiece | 45 |
| 4.2.2 | Electromagnet current | 45 |
| 4.2.3 | Working gap | 46 |
| 4.2.4 | Abrasive mesh size | 46 |
| 4.3 | Design of experiments | 46 |
| 4.3.1 | Workpiece detail | 48 |
| 4.4 | Response surface regression analysis | 51 |
| 4.5 | Results and Discussion | 58 |
| 4.5.1 | Effect of rotational speed of workpiece | 58 |
| 4.5.2 | Effect of magnetizing current | 59 |
| 4.5.3 | Effect of working gap | 60 |
| 4.5.4 | Effect of abrasive mesh size | 62 |
| 4.6 | Confirmation experiments for validation of model | 64 |
| 4.7 | Optimization of process | 65 |
| 4.8 | Performance evaluation of turning type magnetorheological process with finishing time | 67 |
| 4.9 | Conclusion | 69 |

| | |
|---|----|
| 5. Conclusion and scope for the future | |
| 5.1 Conclusions | 70 |
| 5.2 Scope for the future work | 71 |
| 6. References | 72 |

List of Figures

| | | |
|-------------|---|----|
| Figure 1.1 | a) Schematic and (b) actual photograph of magnetorheological fluid polisher with vertical wheel | 4 |
| Figure 1.2 | Magnetorheological effect (a) absence of magnetic field, (b) presence of magnetic field strength H , and (c) at magnetic field H and applied shear strain C | 4 |
| Figure 1.3 | Schematic Magnetic abrasive Machining | 5 |
| Figure 1.4 | Mechanism of magnetic abrasive finishing and Forces acting on abrasive grain due to MAF | 6 |
| Figure 1.5 | Mechanism of magnetorheological abrasive flow finishing Process | 7 |
| Figure 1.6 | Finishing action on a single profile in the presence of external magnetic field | 7 |
| Figure 1.7 | Photograph of the experimental setup used in finishing and Mechanism of Magnetic Float Polishing process | 8 |
| Figure 1.8 | Experimental setup of magnetorheological jet finishing and Jet snapshot images | 9 |
| Figure 1.9 | Experimental setup of ball-end type of magnetorheological finishing process and MR polishing fluid delivery system | 10 |
| Figure 1.10 | Mechanism of ball-end type of magnetorheological finishing Process | 11 |
| Figure 2.1 | Effect of electric current and weight of magnetic abrasive on normal force | 12 |
| Figure 2.2 | Schematic diagram of particles (a) in absence of magnetic field and (b) chain formation in magnetic field H | 19 |
| Figure 2.3 | Flow diagram of methodology steps followed for completing the present objectives | 23 |
| Figure 3.1 | Schematic diagram of turning type MRF experimental setup | 25 |
| Figure 3.2 | Photograph of turning type MRF experimental setup | 25 |
| Figure 3.3 | Schematic diagram of mechanism of material removal | 26 |
| Figure 3.4 | Flow chart of different phases in Maxwell ansoft V13 for analysis of magnetic flux density | 27 |

| | | |
|-------------|---|----|
| Figure 3.5 | Electromagnet model of turning type MRF flat tool tip with external cylindrical surface | 28 |
| Figure 3.6 | The magnetic flux density distributions at flat type tool tip at different working gap | 29 |
| Figure 3.7 | Magnetic field density distribution at distance across the flat tool tip surface | 30 |
| Figure 3.8 | Magnetic flux density distribution at curve type tool tip at different working gap | 31 |
| Figure 3.9 | Magnetic field density distribution at distance across the curve tool tip surface | 32 |
| Figure 3.10 | Surface roughness profiles of (a) initial, (b) flat tool tip surface and (c) curve tool tip surface after 90 minutes of finishing on external surface of cylindrical mild steel workpiece at rotational speed of 443 rpm, electromagnet current of 2A and working gap of 0.5 mm | 34 |
| Figure 3.11 | 3D CAD model of MRF tool | 37 |
| Figure 3.12 | Drawings of MRF tool parts | 37 |
| Figure 3.13 | CAD model of stirring machine | 38 |
| Figure 3.14 | Photograph of MRF fluid stirring machine | 39 |
| Figure 3.15 | Photograph of permanent mould die punch | 40 |
| Figure 3.16 | a) Front view of the workpiece held in a four jaw chuck and gap maintained between the detachable tool tip and cylindrical surface of the workpiece, (b) top view of the workpiece with MRF fluid filling the gap between tool tip and cylindrical surface during the finishing Process | 41 |
| Figure 3.17 | Roughness profiles of cylindrical surface of the permanent mould punch (a) before and (b) after 120 minutes of finishing | 42 |
| Figure 3.18 | Mirror image of cylindrical surface of permanent mould punch (a) before and (b) after 120 minutes of finishing | 43 |
| Figure 4.1 | CAD model and drawing of workpiece | 48 |
| Figure 4.2 | Photograph of cylindrical workpiece with dovetail groove | 57 |
| Figure 4.3 | Effect of rotation speed of workpiece on percentage reduction in Ra value | 58 |
| Figure 4.4 | Schematic of effect of rotational speed on CIP chains | 59 |

| | | |
|-------------|--|----|
| Figure 4.5 | Effect of magnetizing current on percentage reduction in Ra value | 59 |
| Figure 4.6 | (a) Contour and (b) 3D plot of the variation of the %Ra value with working gap and workpiece rotational speed | 60 |
| Figure 4.7 | Effect of working gap on percentage reduction in Ra value | 61 |
| Figure 4.8 | Effect of abrasive mesh size on percentage reduction in Ra value | 62 |
| Figure 4.9 | Schematic of CIP chains with abrasives | 62 |
| Figure 4.10 | Surface roughness profile of (a) initial and (b) after finishing at current 3.5A, gap 1mm, rotation speed 300rpm and abrasive 600 mesh size for 60 minutes (Table 4.5, Exp no. 2) | 63 |
| Figure 4.11 | SEM micrograph at 1000x (a) initial and (b) after finishing at current 3.5A, gap 1mm, rotation speed 300rpm and abrasive 600 mesh size for 60 minutes (Table 4.5, Exp no. 2) | 64 |
| Figure 4.12 | Surface roughness profile of (a) initial and (b) after finishing at optimum parameter as rotational speed of tool core 150 rpm, magnetizing current 3.5A, gap 0.5mm and abrasive mesh size 600 | 66 |
| Figure 4.13 | SEM micrograph at 1000x (a) initial and (b) after finishing at optimum parameter as rotational speed of tool core 150 rpm, magnetizing current 3.5A, gap 0.5mm and abrasive mesh size 600 | 66 |
| Figure 4.14 | Effect of finishing time on surface roughness value | 67 |
| Figure 4.15 | Surface roughness profiles of (a) initial and (b) after finishing at best condition current 3.5A, gap 1mm, rotation speed 300rpm and abrasive 600 mesh size | 68 |
| Figure 4.16 | SEM micrograph at 1000x (a) initial and (b) after finishing at best condition current 3.5A, gap 1mm, rotation speed 300rpm and abrasive 600 mesh size | 69 |

List of Tables

| | | |
|------------|--|----|
| Table 2.1 | Surface roughness results | 14 |
| Table 3.1 | Assigned parameters with material and relative permeability to electromagnet model | 27 |
| Table 3.2 | Magnetic flux density with flat tool tip at different working gaps in Tesla B(T) | 29 |
| Table 3.3 | Magnetic flux density with curve tool tip at different working gaps in Tesla B(T) | 30 |
| Table 3.4 | Technical specification of the present lathe machine | 34 |
| Table 4.1 | Composition of MR polishing fluid | 45 |
| Table 4.2 | Coded levels and corresponding actual values of the process Parameters | 47 |
| Table 4.3 | Experimental parameters and conditions | 47 |
| Table 4.4 | Plan of experiments | 49 |
| Table 4.5 | Summary of response | 50 |
| Table 4.6 | Sequential model sum of squares | 52 |
| Table 4.7 | Lack of fit tests | 52 |
| Table 4.8 | ANOVA for percentage change in Ra | 53 |
| Table 4.9 | Other ANOVA parameters | 54 |
| Table 4.10 | Factor coefficients | 54 |
| Table 4.11 | ANOVA for % change in Ra after dropping the insignificant Terms | 56 |
| Table 4.12 | Other ANOVA parameters after model reduction | 56 |
| Table 4.13 | Factor coefficients after model reduction | 57 |
| Table 4.14 | Percentage contribution of process parameter in final response of Ra | 57 |
| Table 4.15 | Confirmation tests and their comparison with the results | 64 |
| Table 4.16 | Optimum conditions for maximizing the percentage change in surface roughness (ΔRa) | 65 |

Nomenclature

R_a = Average roughness value

R_z = Average distance between the highest peak and the lowest valley in each sampling length

R_q = Root mean square value

R_{a_i} = Initial average roughness value

R_{a_f} = Final average roughness value

R_a = change in average roughness value

% R_a = Percentage change in roughness

Greek Symbols

μ = Micro

Acronyms

| | |
|-------|--|
| I | = Current |
| N | = Rotational speed of workpiece |
| A | = Abrasive mesh size |
| Z | = Working gap |
| RMS | = Root mean square |
| DoF | = Degree of freedom |
| 2FI | = Two factor interaction |
| S.D | = Standard deviation |
| C.V | = Coefficient of variance |
| C.I | = Confidence interval |
| VIF | = Variance inflection factor |
| CIP | = Carbonyl iron particles |
| AFM | = Abrasive flow machining |
| CMP | = Chemo mechanical polishing |
| MAF | = Magnetic abrasive finishing |
| MRF | = Magnetorheological finishing |
| MFP | = Magnetic float polishing |
| MJF | = Magnetorheological jet finishing |
| MRAFF | = Magnetorheological abrasive flow finishing |
| BEMRF | = Ball end magnetorheological finishing |
| MRP | = Magnetorheological polishing |
| SEM | = Scanning electron microscope |
| RSM | = Response surface method |
| ANOVA | = Analysis of Variance |

Chapter 1

Introduction

1.1 Introduction

This chapter includes the introduction and need of the magnetorheological fluid based finishing. It discusses the various types of magnetic assisted processes. The chapter also discuss about the magnetorheological fluid and the mechanism of material removal.

Any manufacturing process can be use to make the product i.e. casting, forging, welding, forming or machining is required to finish. Mostly time finishing cost, approach to 10-15% of product cost [Jain, 2008]. Surface finish is necessary to improve the product quality, precision fits and high strength applications. There are numbers of processes which are used to finish the surfaces of the parts. The machining parameters mainly responsible to controls of surface and/or sub surface defects such as micro or macro cracks, heat affected zone, micro structural changes [Jain, 2008]. The finishing processes mainly divided in two categories: conventional finishing processes (grinding, honing, and lapping) and advanced finishing processes (abrasive flow machining, magnetorheological machining, elastic emission machining, chemo-mechanical machining polishing). In conventional finishing processes size and shape of product is the main problem. No control on the forces acting during the finishing operation is also responsible to low grade of finishing. The traditional processes cannot finish the 3D complex geometries; small holes having diameter $< 2\text{mm}$ [Jain, 2009]. Due to these limitations the advanced finishing processes are developed in which in process externally controllable forces acting on the workpieces, finishing of complex shape workpiece are possible. The advanced finishing processes can be divided into two groups: no externally control on the workpiece forces and forces controlled on workpiece. Forces can be controlled in magnetic assisted machining by varying DC supply if using electromagnet and by changing working gap if using permanent magnet. By controlling the forces the significant % change in surface finish can be achieved. The major problem to finish

the complex geometries is that it cannot be defined the relative motion of tool with respect to the workpiece surface. Thus some processes are developed in which loose bonded abrasives are directly flow over the work surface to be finished. Because of no control on the finishing forces, these processes impart surface and subsurface damages [Jain, 2009]. Many advanced finishing processes have been developed to tackle these issues. Magnetorheological fluid assisted processes are also developed for surface finishing because of easily control on the process forces, so product can be finish with close tolerances and also achieve defect free surface. Many new processes are developed in which forces can be controlled by externally. Few of them are magnetorheological finishing (MRF), magnetorheological jet finishing (MRFJ) [Kordonski *et al.*, 2006], magnetorheological abrasive flow finishing (MRAFF) [Jha and Jain, 2004], magnetorheological abrasive honing (MRAH) [Sadiq and Shunmugan, 2010] and ball end magnetorheological finishing [Singh *et al.*, 2011]. Firstly, magnetorheological finishing was invented and developed by collaboration of some international group at center for optics manufacturing in mid 1990's. After perform the experiments it is concluded the MR finishing was capable of polishing glass, zinc selenide, sapphire, quartz and silicon nitride. In 1995 William Kordonski developed a new prototype of MRF finishing machine with vertical wheel. The MRF was commercialized by QED Technology, Inc. in 1997 [Harris, 2011]. These above finishing were only able to finish the concave, convex, flat and spherical optical components. Because the commercialization of the technology research on MRF was start all over the world. The researchers developed the new setups which can finish the 3D surfaces and freeform surfaces also.

1.2 Conventional Finishing Process

1.2.1 Grinding Process

It is most commonly process which is used to finish the workpiece. The material removal mechanism in this process is abrasive action. A grinding wheel is used for this purpose which consist the abrasive particles held together by a bonding material. Better surface finish and dimensional accuracy can be achieved by the grinding.

1.2.2 Lapping Process

Lapping is mainly done on mating surfaces. Abrasive compound or solid bounded can be used for finishing. Material removal mechanism in this process is also abrasion. Lapping slurry is made up of mixing of diamond, silicon carbide, aluminum oxide with oil or water. In lapping process the surface finish is depends on the speed and pressure.

1.2.3 Honing Process

Honing process is used to finish the cylindrical surfaces i.e. internal as well as external. Honing tool made up of abrasive particles which are responsible for the finishing. Two combined motions (rotary and translator) are given to the honing tool. Honing process mainly performed as final operation which helps to correct error that has occurred in previous machining processes.

1.3 Advanced Finishing Processes

1.3.1 Magnetorheological Finishing (MRF)

Magnetorheological finishing process was developed to finish the brittle materials such as glass which tends to crack during machining by other finishing processes. This process was developed by the center for optics manufacturing at Rochester, N.Y for high-precision lenses. MR polishing fluid (smart fluid) is used in this process as a tool. Main constituents of MR polishing fluids are carbonyl iron particles, non-magnetic carrier medium, abrasives and additives. The main process parameter which directly effects the surface finish of workpiece are working gap between workpiece and tool tip, magnetic field strength, abrasive particles shape and size, wheel speed, workpiece properties and CIPs iron particles size. This finishing process is used for finishing optical glasses, glass ceramics, plastics and some non-magnetic metals. The finishing process is capable to produce surface finish of the order of 10-100 nm peak to valley height, and 0.8 nm RMS value in finishing optical lenses [Jain, 2008].

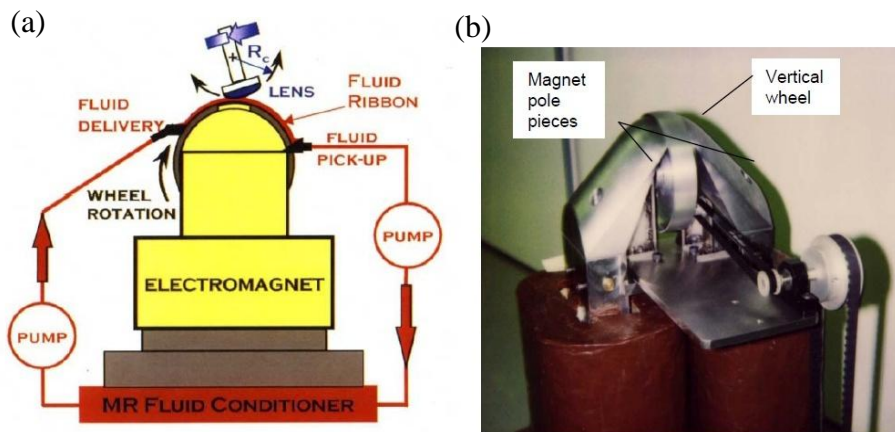


Figure 1.1: (a) Schematic and (b) actual photograph of magnetorheological fluid polisher with vertical wheel [Harris, 2011]

Magnetorheological fluid consists of a magnetic particle (such as carbonyl iron particles) and abrasive particles dispersed in a non magnetic carrier such as silicone oil, mineral oil or water. When magnetic field is not applied the MR fluid follows newtonian behaviour. To observe the magnetorheological behaviour apply magnetic field to the MR fluid. The particles were arbitrarily spread in the absence of magnetic field as shown in Fig. 1.2 (a). In presence of magnetic field CIP's forms chains and hold the abrasive between the chains shown in Fig. 1.2 (b). The increase in the resistance to an applied shear strain γ due to the yield stress as shown in Fig. 1.2 (c).

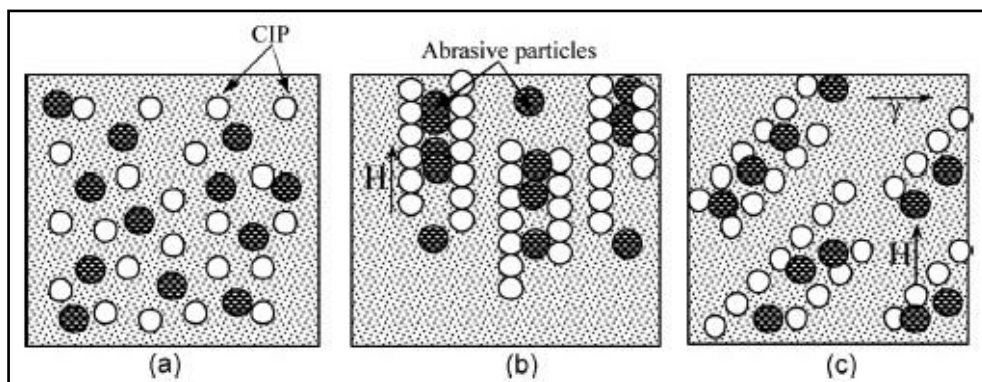


Figure 1.2: Magnetorheological effect (a) absence of magnetic field; (b) Presence of magnetic field strength H , and (c) at magnetic field H and applied shear strain C [Jha and Jain, 2005]

1.3.2 Magnetic Abrasive Finishing

This process is more suitable for large size flat workpiece of hard and brittle materials. In this process ferromagnetic abrasive particles are used. MAF process in which finishes action is controlled by magnetic field across the machining gap between the workpiece and electromagnet pole. The experimental setup of MAF is as shown in Fig. 1.3. In MAF process two permanent magnets are used around the workpiece. The ferromagnetic abrasive particles were introduced in the working gap. The mechanism of magnetic abrasive finishing process is shown in Fig. 1.4. In the presence of magnetic field, magnetic abrasive particles form a brush for finishing the workpiece [Shinmura *et al.*, 1985]. The flexible magnetic abrasive brush behaves as a multi point cutting tool for removing the material in the form of chips. The normal component force due to magnetic abrasive particles is responsible for the penetration of magnetic abrasive particles onto the workpiece. The magnetic abrasive finishing process is used to finishing the external and internal surfaces of the tubes or a flat surface made from magnetic/non magnetic material.

The magnetic field acts as a binder. MAF is used for polishing and removal oxide layer from high speed rotating shafts. The material removal rate and finishing rate depend on the workpiece circumferential speed, magnetic flux density, working gap and type and volume fraction of abrasives. Finishing of stainless steel rollers using MAF process to obtain final Ra of 7.6nm at an average finishing rate of 7.08 nm/s. MAF is also used for micro-deburring with permanent magnet.

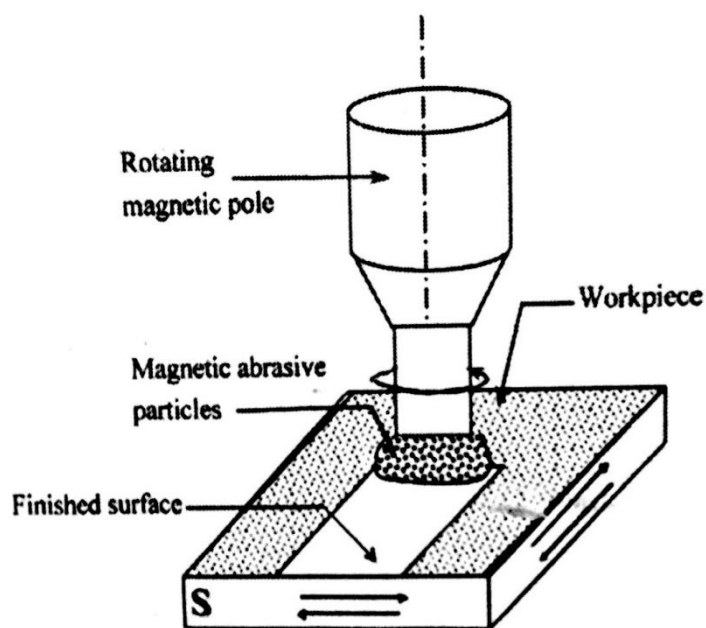


Figure 1.3: Schematic magnetic abrasive machining [Jain, 2008]

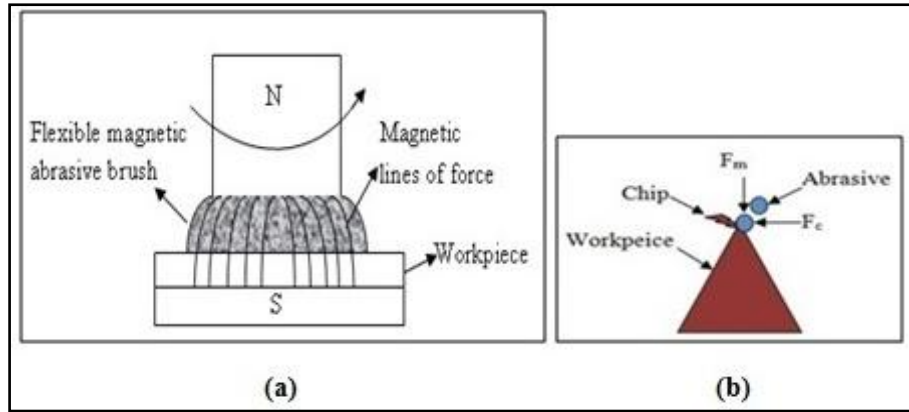


Figure 1.4: (a) Mechanism of magnetic abrasive finishing (b) forces acting on abrasive grain due to MAF [Jain, 2009]

1.3.3 Magnetorheological Abrasive Flow Finishing

It is a new hybrid process termed as magnetorheological abrasive flow finishing (MRAFF) this process is developed by Jha and Jain in 2004. It is modified from the AFM process. In AFM process the abrading forces are not controllable. This process is a combination of AFF and MRF. The MRAFF gives the same flexibility in the process but now with controllable abrading forces. Abrasive mixed viscous base medium acts as a “self deformable stone”. This process is mainly developed to finish intricate internal and external shapes or where very difficult to reach. CIP’s chain holds the abrasive particles tightly penetrate in work-piece and shear the peaks from it. The material removal from the workpiece is directly depends on the extrusion pressure and magnetic field which provides the strength to MR polishing fluid. The external magnetic field is decided up to which level the magnetic particles stiffened and the viscosity of fluid [Seok *et al.*, 2009; Kordonski *et al.*, 1999]. The MRAFF process is used to finish the complex internal and external geometry, optical flats, spheres etc. The best finish obtained by the present setup is 30 nm on stainless steel workpiece. The mechanism of Magnetorheological abrasive flow finishing process is as shown in Fig. 1.5. MRAFF process consisted of CIPs particles, abrasive particles along with the base media. The finishing action on a single profile due to external magnetic field is as shown in Fig. 1.6. As magnetic field increased, CIP’s chains hold abrasive particle strongly which results high finishing.

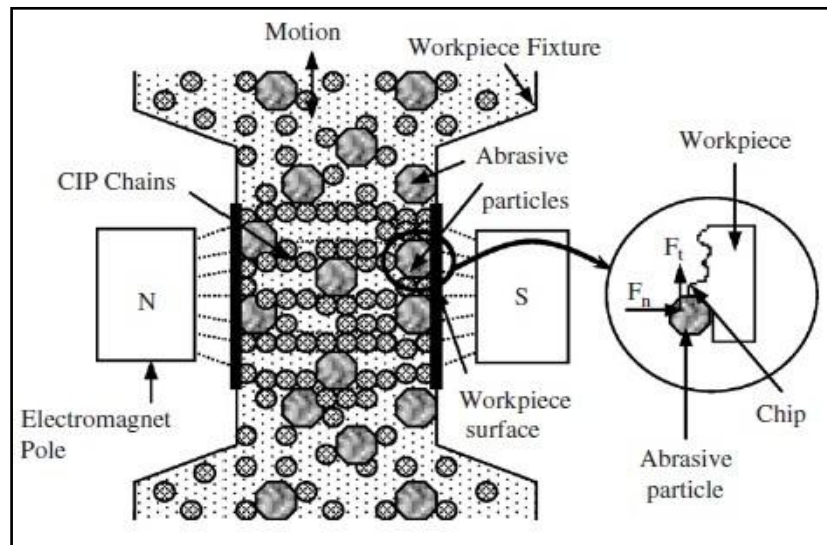


Figure 1.5: Mechanism of magnetorheological abrasive flow finishing process [Jha and Jain, 2004]

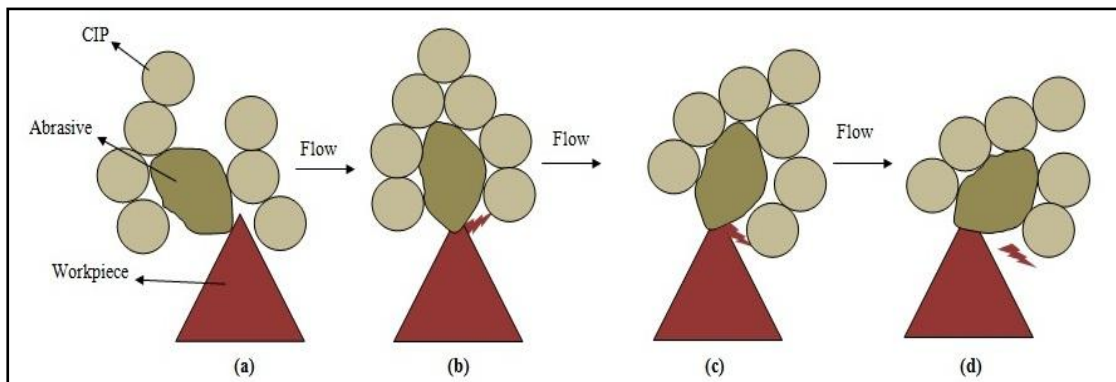


Figure 1.6: Finishing action on a single profile in the presence of external magnetic field (a) abrasive grain along with CIP chains approaching roughness peak (b) abrasive grain takes a small cut on roughness peak (c) abrasive grain takes another small cut on the roughness peak (d) abrasive grain crossing the roughness peak after removing a microchip during cutting action [Jha and Jain, 2004]

1.3.4 Magnetic Float Polishing

The various types of finishing processes have been developed for finishing of either flat surfaces, cylindrical surfaces or their combinations leading to complex 3-D surfaces. This process is mainly used for the finishing of the rollers and ceramics balls which used in bearings with the help of fine abrasive particles. The experimental setup and mechanism of magnetic float polishing process is shown in Fig. 1.7. MFP finishing process is based upon the ferro-hydrodynamic behavior of magnetic fluid that rise a non-magnetic float and abrasive particles suspended in it by the application of magnetic field. The drive shaft is moved downward to contact the spherical balls and press them downward to reach the desired force level. The balls are polished by means of a relative motion between the balls and the abrasive particles under the influence of the force. Magnetic Float polishing is used to finish 9.5 mm diameter Si_3N_4 balls. The surface finish obtained was 4 nm Ra and 40 nm Rmax. The best sphericity obtained of the Si_3N_4 balls were 0.15 to 0.2 μm [Jha and Jain, 2005].

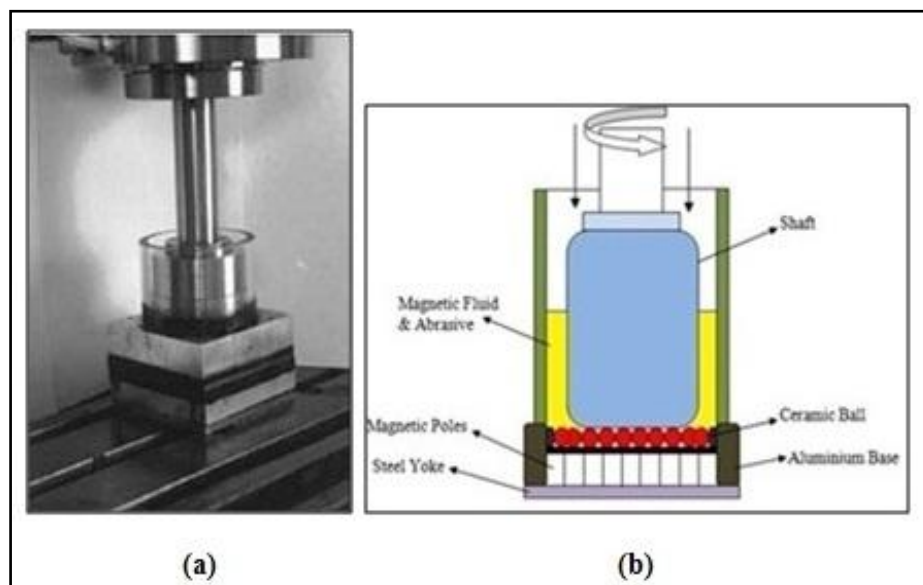


Figure 1.7: (a) Photograph of the experimental setup used in finishing Si_3N_4 balls by small batch Magnetic float polishing apparatus (b) mechanism of magnetic Float polishing process [Jiang and Komanduri, 1998; Komanduri *et al.*, 1999]

1.3.5 Magnetorheological Jet Finishing

The Magnetorheological jet finishing have been newly developed for finishing of parts with a freeform optics, cavities, steep concave etc. The water jet finishing is converted into MRF process in which MR fluid jet is used for finishing the internal surface of work-piece and magnetic axial magnetic field is applied when it flows out of the nozzle. The Magnetorheological jet finishing is used to finish internal surface of the work material. The jet snapshot image of magnetic abrasive jet finishing (velocity- 30 m/s, nozzle diameter- 2 mm) is as shown in Fig. 1.8(b) [Kordonski *et al.*, 2006]. The jet of water loses its coherence when passes through the nozzle. When the magnet is off, the jet of MR fluid passes through nozzle losses its coherence due to its high viscosity. When the magnetic is on, the stable jet of MR fluid passes through the nozzle with low viscosity and high velocity jet.

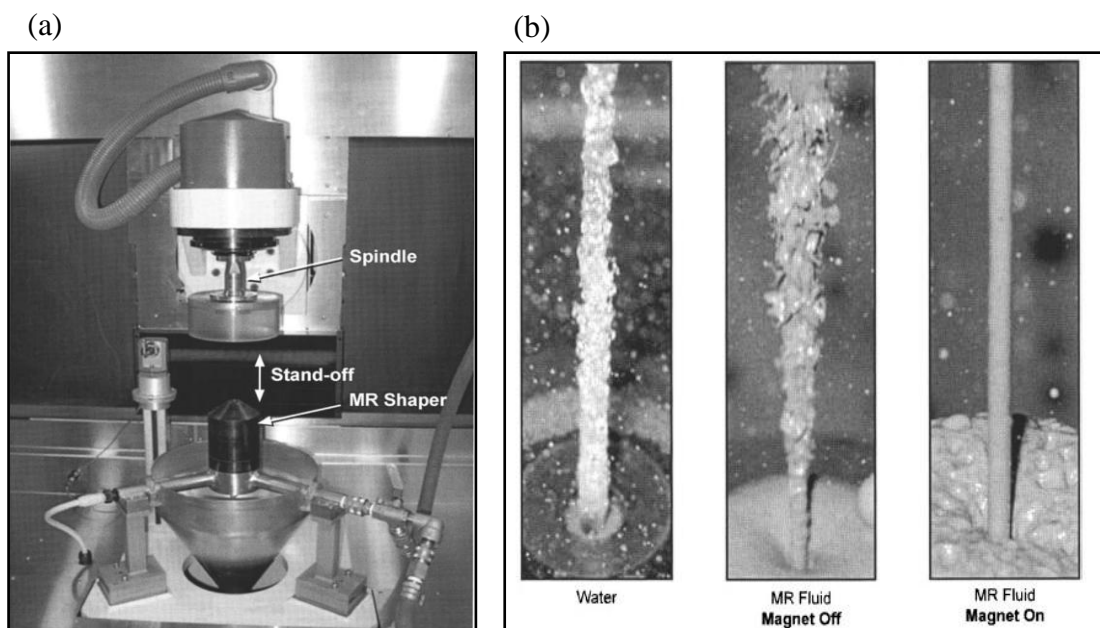


Figure 1.8: (a) Experimental setup of magnetorheological jet finishing and (b) jet snapshot images [Kordonski *et al.*, 2006]

1.3.6 Ball end type Magnetorheological Finishing

Forces can be easily and better controllable in BEMRF process and finish the 3D work-piece very precisely [Singh *et al.*, 2012]. The experimental setup of BEMRF is shown in Fig. 1.9. Magnetorheological fluid consists of carbonyl iron powder, abrasive particles, water and additives [Sidpara *et al.*, 2009] form a chain like structure for precise finishing of the work material. The material removal takes place by the action of the shearing stress between the abrasive and work material.

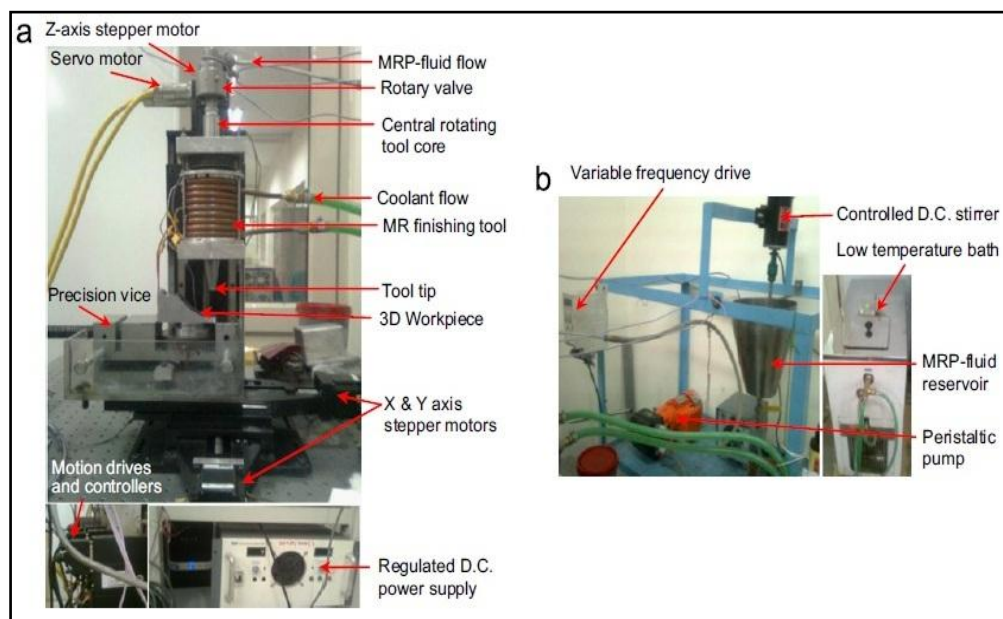


Figure 1.9: Experimental setup of ball-end type of magnetorheological finishing process (a) MR polishing (MRP) fluid delivery system [Singh *et al.*, 2012]

The mechanism of material removal during the BEMRF process is as shown in Fig. 1.10. Due to the higher shear strength, CIP's chains hold abrasive particles more tightly and robustly like a single body during the time of finishing. In the presence of the high magnetic field abrasive particle easily penetrate in the peaks as shown in Fig. 1.10 (a). Due to the high magnetic field the yield strength of MRP fluid is increases, which helps to remove the peaks in the form in microchips as shown in Fig. 1.10 (b). When continuous feed rate is given to the workpiece than material removal is due to abrasion as shown in Fig. 1.10(c).

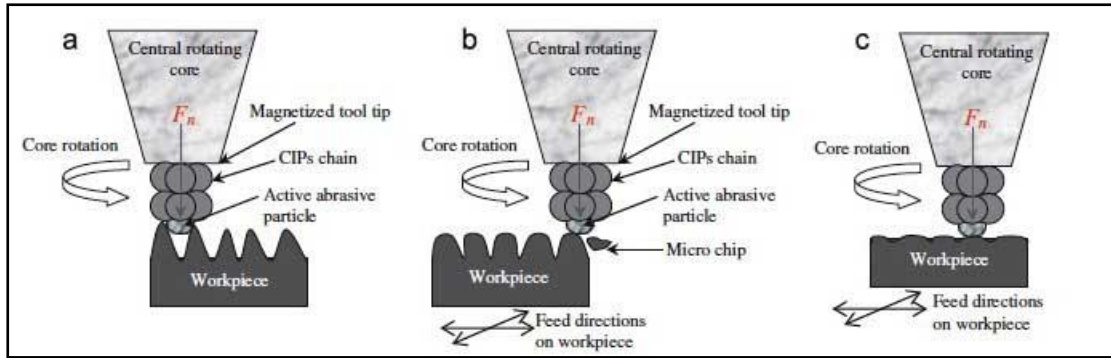


Figure 1.10: Mechanism of ball-end type of magnetorheological finishing process

[Singh *et al.*, 2013]

1.4 Advantage of Advanced Finishing Processes

- Closer tolerances can be achieved.
- Increase the life of the work material.
- Better sealing capabilities.
- Decreasing the wear and friction losses.
- Used for finishing of internal and external surfaces.
- Reduces the surface defects (such micro cracks, cavity etc.).
- Capable to accessing hard to reach areas.
- These processes are force controllable processes.

1.5 Application of Advanced Finishing Processes

The advanced finishing processes have its wide applications in finishing of automotive parts (such as bore of an internal combustion engine, connecting rod, cam shaft lobes, bearing race, fuel injector component etc.) medical instrument, electronic component, finishing of dies, turbine component, aerospace, automotive and machine tool manufacturing, packing seal manufacturing industries, valve and pipe manufacturing industries etc.

Chapter 2

Literature Review

2.1 Literature review

In this chapter literature review of various authors in the field of advanced nano finishing processes (for ferromagnetic and non ferromagnetic workpiece) and their observations are drawn in brief from the papers and are represented for better understanding.

Mori et al. (2003) carried out the effect of electric current on the forces while working on magnetic abrasive polishing apparatus for finishing of SUS-304 stainless steel. The authors founds that with the increase in electric current from 0.5-5 Amp, the normal force increases, whereas with the increase in weight of magnetic abrasive, the normal force and tangential force increases simultaneously as illustrated in Fig. 2.1.

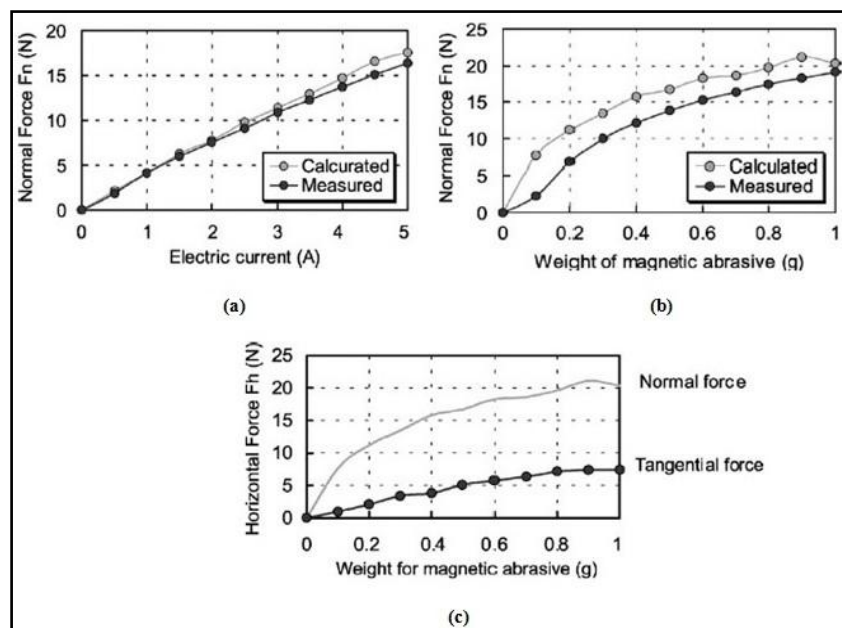


Figure 2.1: (a) Normal force v/s electric current (b) Normal force v/s weight of magnetic abrasive (c) Horizontal force v/s weight of magnetic abrasive (Mori et al., 2003)

Yin and Shinmura (2004) compare the performance of surface roughness and deburring on three different material by using vibration-assisted magnetic finishing process. The finishing fluid was prepared with the mixture of iron particles, WA

magnetic alumina and straight oil type grinding fluid. The experiments was conducted on magnesium alloy (AZ31B), stainless steel (SU304) and brass (C2680). Better deburring and % change in reduction in surface roughness was found on magnesium alloy (AZ31B) as compared to other 2 materials.

Yamaguchi and Shinmura (2004) performed their experiment on the magnetic assisted finishing process for finishing of alumina ceramic tube. The experimentation was performed by using different iron particle (150, 330 and 510 μm), diamond abrasive (0-1, 2-4, 4-8 and 8-12 μm) and lubricant (0.1, 0.2, 0.25, 0.3 and 0.35 ml). The results concluded that with the use of iron particle (330 μm), diamond abrasive (0-1 μm) and lubricant (30 ml), the surface roughness reduces to 0.02 μm .

Jha and Jain (2004) designed and developed a new type finishing process (MRAFF) for intricate internal geometries by combined exiting two processes magnetorheological finishing (MRF) and abrasive flow finishing (AFM). Main advantage of this process was that the external forces can be easily controlled by varying the magnetic field. To see the process capability the experiments were performed on the stainless steel workpieces by varying the magnetic field. The fluid was prepared with 20% CIP's, 20% Sic abrasives and 60% viscoplastic base fluid. The surface roughness was measured after every 200 cycles on different-2 magnetic field. Authors also observed that there was no surface roughness change at no magnetic field and abrasion marks and direction of motion was clearly observed at high magnetic field.

Jha and Jain (2006) studied the effect of various grades of CIPs particles (CS and HS) on the finishing by using MRAFF when finishing of stainless steel. The fluid used for finishing was a mixture of 20% CIPs, 20% SiC abrasive powder and 60% visco plastic base medium. The better results achieved when finishing was done with CIPs (CS) with Sic-800 mesh size grade as illustrated in Table 2.1.

Table No. 2.1 Surface roughness results (Jha and Jain, 2006)

| Expt. No. | CIP dia. (D_{CIP}) (μm) | SiC dia. (D_{SiC}) (μm) | D_{CIP}/D_{SiC} | Initial Ra (μm) | Final Ra (μm) | ΔRa^a (μm) | $\%\Delta\text{Ra}$ |
|-----------|--|--|-------------------|------------------------------|----------------------------|---------------------------------------|---------------------|
| 1. | 18.0 (CS) | 19.00 | 0.95 | 0.32 | 0.09 | -0.23 | -17.87 |
| 2. | 18.0 (CS) | 12.67 | 1.42 | 0.28 | 0.17 | -0.11 | -39.28 |
| 3. | 18.0 (CS) | 7.50 | 2.40 | 0.31 | 0.23 | -0.08 | -25.80 |
| 4. | 3.5 (HS) | 19.00 | 0.18 | 0.26 | 0.23 | -0.03 | -11.54 |
| 5. | 3.5 (HS) | 12.67 | 0.28 | 0.28 | 0.24 | -0.04 | -14.28 |
| 6. | 3.5 (HS) | 7.50 | 0.47 | 0.25 | 0.24 | -0.01 | -4.00 |

Sadiq et al. (2009) developed a new magnetorheological finishing process which is used to finish the external curved surfaces and studied the effect of magnetic field, initial surface finishing roughness, workpiece rotation and process duration on the final surface roughness and metal removal. The experiments were conducted on aluminum and austenite stainless steel workpieces. The surface roughness was greatly affected by changing the magnetic field. The initial surface roughness of workpiece, process duration and rotation speed also responsible to achieve the low surface roughness.

Sadiq et al. (2009) studied the effect of magnetic field and process duration on the surface finish obtained on magnetic and non-magnetic specimens. The authors proposed a method to improve the finishing of non-magnetic surfaces. When the experiments were conducted by new proposed method the percentage change in roughness is significantly increases to 41.7% at 0.65 T corresponding to 2A. The

proposed method also increase the surface roughness to 43.5% from 24.2% for process duration.

Wang and Lee (2009) was studied the effect on surface roughness by changing the base fluid of MR fluid in magnetic abrasive finishing with silicone gel. MR fluid prepared with silicone gel was recycled after stirring it more than 15 times which was not possible with previous fluid that was waste after only one time used. To see the effect the experiment was conducted on mild steel rod. The surface roughness reduced from Ra 0.677 μm to 0.1 μm in just 10 min and 0.038 μm after 30 min. The surface roughness improvement at 90% level even after finishing 15 workpieces. Silicone as a base fluid had self-sharpening, self-adaptability, controllability capabilities and recycled.

Sadiq and Shunmugam (2010) performed experiments to finish the mild steel (AISI 1020) and stainless steel (SS 316L) on MR honing process at a different magnetic flux density with the rotation speed of 310 RPM. From results it can be seen that a very little change in Ra (6.7% at 0T, no change at 0.65T) when finishing of the mild steel material, other side a significant improvement in surface finish (41.7% at 0.65T) and (43.5% at 20 min) when stainless steel is finished.

Das et al. (2010) developed a new polishing method for internal finishing of pipes called rotational magnetorheological abrasive flow finishing (R-MRAFF). In this process two main motion were given to the fluid rotational as well as reciprocating. For best results the experiments were design with the help of design of experiments and to see the effect of each parameter response surface regression analysis was used. The magnetic flux density and forces analysis done with the help of Maxwell anssoft software. The fluid was prepared with 26.6 vol.% of electrolytic *Fe* powder and 13.4 vol.% SiC abrasive with the 60% base medium (paraffin oil (48 vol.%) and AP3 grease (12 vol.%)).The most significant factor for finishing was rotating speed and second was extrusion pressure. The minimum surface roughness was achived 16 nm at magnet rotational speed 149 rpm, extrusion pressure 40 bar and finishing cycle 1200.

Singh et al. (2010) designed and developed a new setup (ball end magnetorheological finishing) which is used to finishing on flat as well as 3D surfaces of ferromagnetic or

non-ferromagnetic materials. They also studied the effect of the shape and size of the finishing spot in contact with the workpiece surface by varying the working gap for the same magnetizing current. The process performance is greatly depend on magnetic nature of workpiece material, working gap, and magnetizing current.

Singh et al. (2011) studied the effect of finishing time on surface roughness, root mean square and R_{\max} value of Fused silica Glass when it machining with the Ball-End magnetorheological finishing. MR fluid was prepared with (by volume) 30% of CIPs, 10% of cerium oxide cerox 1663 abrasive powder (1-2um), carrier fluid demonized water. The surface roughness is decreased to $R_a = 0.14$, $RMS = 0.26$ and $R_{\max} = 0.94$ from 0.74 nm, 1.03 nm, 5.13 nm respectively at 2.4V with 5 cycles of 30 minutes each.

Sidpara et al. (2011) studied the effect of process parameters like concentration of magnetic particles and abrasive particles, carrier wheel speed and initial surface roughness on surface finish and material removal rate in MRF of single crystal silicon blank. At last optimization study is performed to select the range of the independent parameters. It is found that 39.58% CIPs, 5.07% abrasives and 298.36 rpm of carrier wheel speed are required to minimize final R_a and maximum MRR of single crystal silicon blank with use of permanent magnet (N48 grade). Deionized water is used as carrier fluid.

Jang et al. (2012) proposed new deburring process in conjunction with magnetorheological fluid and this process applied successfully to remove metal burrs with a height of 200 μm and thickness of 1 μm in micro-moulds with extensive yielding and abrasive wear. The average R_a of brass decreased from 192nm to 34nm after 4 min of processing. For stainless steel, the average R_a decreased from 379.8nm to 147.1nm.

Hong et al. (2012) performed their experiments to finish the alumina reinforced zircon ceramics (used in dental application 3YTZP/ Al_2O_3 -20%) with the help of MR finishing process. MR fluid is prepared with 50% CIP's, 48% abrasive slurry with diamond abrasives and glycerin is used as a stabilizer. The process parameters are (speed-200 and 300 rpm, magnetic field- 3.8,4.7,5.5 and 6.1 KA/m, Time- 20,30,40

and 60 min). The surface roughness decreases from 0.272 μm to 1.96 nm on 300rpm, magnetic field-3.8 KA/m and 60 min.

Singh et al. (2013) investigated the effect of the MRF fluid composition on the performance of BEMRF process. The authors selected Sic abrasives with various mesh sizes to performance analysis of the process in terms of change in surface roughness of ferromagnetic workpiece. In this investigation they found that the process with MRP fluid composition 5% volume of Sic800 and 15% volume of Sic1200 were less efficient and process perform very effectively with 15% volume of Sic400 in MRP fluid. The authors also observed that the with the increase in percentage of abrasive particle the bonding strength of CIP chains reduced because there are more abrasives than CIP's so weak bond exist. Authors also developed mathematical models to see the active abrasives and active CIP's in working gap and total numbers of CIP chains formed and number of active abrasives per chain can also be calculated.

Jiao et al. (2013) investigated the new modified magnetic compound fluid (MCF) wheel which was used to finishing the fused silica glass. The author developed the setup with permanent ring shaped magnet which is used for generate magnetic field. The author compared the new modified MCF wheel with unmodified MCF wheel by perform experiments and see the results by compare the material removal and surface roughness. The MCF slurry composition was CIP's 58%, abrasive (cerium oxide) 12% and magnetic fluid 30%. The author also studied the effect of rotational speed and clearance between workpiece and wheel on material removal and surface roughness of workpiece. The final surface roughness was achived by modified and unmodified wheel was $R_a=5.624$ and 14.67 from initial 200nm and material removal was 0.04 mm^3 0.0088 mm^3 respectively at rotation speed 500 rpm and clearance 0.5mm.

Pandey et al. (2013) conducted the study to see the effect of process parameters of BEMRF to finishing the EN31. They selected 3 parameters magnetizing current, working gap and nozzle speed up to 3 levels to design of experiments and apply L-9 orthogonal array. Anova was applied to analyze experimental data to find the contribution of each parameter to achieve final roughness. The MR fluid was prepared with 20% CIP's particle, 20% of Sic abrasives (800 mesh size) and 60% base fluid by

weight. Each experiment was done for the 30 minutes. After the study the optimization parameters to finishing the EN31 on BEMRF was current 1.4A, working gap 0.75mm and nozzle rotation speed 300 rpm. The final roughness was achieved 44 nm from 246 nm.

Pattanaik and Agarwal (2014) designed a new setup to finish the free form surfaces with the help of magnetorheological fluid. Authors modified the pillar type drilling machine and use to finish the freeform surfaces. The study was conducted on copper alloy. Flat and cylindrical surfaces were included in job. The magnetic field is developed with the help of permanent magnet (Nd-Fe-B, N35 grade). The experiments were conducted on different types of condition in which composition of MR fluid, abrasive sizes and rotation speed of workpiece and vessel containing MR fluid. At last concluded that finishing was done in less time when the rotation speed was given to both workpiece and vessel containing MR fluid rather the only to the workpiece. The decrease in surface roughness of flat portion of job was more as compared to the cylindrical surface.

Niranjan and Jha (2014) done experimentation on ball end magnetorheological finishing process to finish the mild steel. The bidisperse MR fluid was used to finish the samples. The results obtained was roughness value decreases to Ra-0.14 μm , Rq-1.19 μm and Rz-1.14 μm .

Niranjan *et al.* (2014) studied on the workpiece surface roughness by changing the MR fluid with new composition of fluid called bidisperse MR fluid. MRPF were prepared with different compositions and compared with each other for best results. They uses two different grades of CIP's (CS and HS grade). The average particle size of CIP's of CS and HS are 6–7 μm and 1.8–2.3 μm , respectively and abrasive particles size 19 μm (SiC). The best results are obtained with this composition CIP 16 vol.% CS grade, 4 vol.% HS grade, 25 vol.% SiC abrasive.

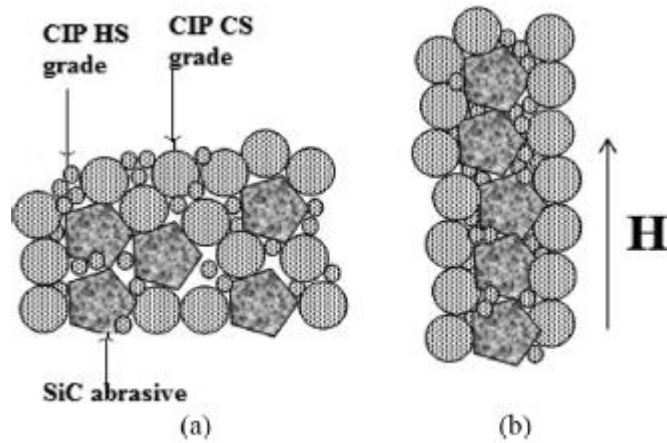


Figure 2.2: Schematic diagram of particles (a) in absence of magnetic field and (b) chain formation in magnetic field H (Niranjan *et al.*, 2014)

Gheisari *et al.* (2014) developed a magnetorheological finishing process for a ultra precision finishing of aluminum work material (cylindrical type). The water based suspension of micron sized diamond particles are used for MR fluid. The optimum parameters were (current- 9A and working gap- 5mm). The initial surface roughness of the work material was 170 nm. The experimentation was conducted in three stages. In first stage, the work material was speed varies from 250-1000. In second stage, the process time varies from 20-100 min. In third stage, the effect of a fast RAM on the surface roughness was considered. The results concluded that the surface roughness value improves by 40 nm with the increase in rotational speed (1000 rpm). The surface roughness value decrease to 42 nm whereas through the raise in finishing time (90 min), the surface irregularity value improves by 78 nm when the fast RAM (with 0.5 m/sec) was applied.

Guo *et al.* (2014) used two types of slurries to remove the single-crystal diamond turning process marks from nickel-phosphorous plated mold material. First slurry containing high quality CIPs and alumina abrasives where as second slurry contains CIP coated with zirconia abrasive particles. From the experimentation that was find out both the slurries was removed scratches from the Ni-P plating surface but slurry containing alumina abrasive left scratches on the work surface and CIPs were also embedded which make surface more worse. The slurry with zirconia coated CIPs perform better than the first slurry there was no scratches or no CIPs embedded on the surface. This results show that MCF polishing slurry is applicable to superfinishing of soft magnetic and non magnetic materials.

Wang et al. (2015) developed a new setup for ultra-finishing the flat workpieces and see the effects of trough speed, work and excitation gap width, particle concentration within the MR fluid on MRR for K9 glass. A permanent magnetic yoke with straight air gap was used for the magnetic field. The polishing setup was demonstrated that the glass surface improved to a roughness value of 1 nm in Ra after 60 min of polishing, from the initial roughness of 127 nm in Ra.

Saraswathamma et al. (2015) used BEMRF process to finish the silicon wafer, by using three parameters magnetizing current, working gap and core rotational speed. The MRP fluid was prepared with deionized water and cerium oxide abrasives. To achieve the maximum reduction in the surface roughness the combination of parameters for experimentation was decided with the help of design of experiments. To see the contribution of different-2 parameters ANOVA was used. Working gap contribute maximum to reduce the surface finish, magnetizing current was on second last and very less contribution given by the core rotational speed. The average Ra of silicon wafer decreased from 457nm to 89.8nm.

Wang et al. (2015) proposed a new method to finish pierced die made with the wire electric discharge machining. When any cavity is cut by the WEDMed, it generates remelted layer which have many surface defects like micro cracks and residual stresses. The pierced die can be polished by this new method to improve the surface quality of the die. The die which was polished made from tool-steel Cr12. Diameter of wire used to cut the die was 0.1mm. A core with permanent magnets was made to finish the pierced die. The MR fluid contains CIP, SiC (3000), water and polyethylene glycol. The working gap was 0.5mm. The finishing was done with the permanent magnet and core by giving reciprocating motion. The final roughness was achieved 0.132 μm at flat surface and 0.278 μm at corner from initial Ra 0.303 μm with 12000 reciprocating motion in 290 min. The experiments were conducted by changing the diameter of wire from which was concluded that to decrease the surface roughness the increase the diameter of wire.

Saraeian et al. (2016) optimized the MAF process parameters working gap, abrasive size and rotation speed for finishing of AISI321 steel by applying full factorial method at three level. The MAF fluid was prepared with CIPs, Sic abrasive and SAE40 oil. The finishing was done on workpiece 50 mm lengths for 20 min. The

three level for rotation speed (355, 500, 1000 rpm), working gap (0.5, 1, 2mm) and abrasive size (100, 200, 300 mesh) was used. The best result was achieved at 1mm gap, 500 rpm and with abrasive size 100 mesh. Working gap is the most effective parameter for finishing after that rotation speed is responsible for finishing. This parameters are only applicable when the initial roughness of workpiece is 0.5036 μ m.

Chen et al. (2016) developed a novel precision MRF process using small ball end permanent magnet polishing head with 4mm diameter. The process is develop to finish the small curvature radius of concave type shapes. Ansoft software was used to check the distribution of magnetic flux density at polishing head which was 93.3%.The fluid was prepared with volume concentration CIP 36%, water based fluid medium 57%, cerium oxide abrasives 6% and stabilizing agent 1%. A device is attached to supply the water in the MR fluid to stable the fluid concentration because the water is evaporate. A flat piece with size 20x10x5 mm of plane glass of fused silica was used to check the feasibility for non-metallic material. The final roughness was achived 0.517nm from initial 214nm at C-axis angular position 65⁰, spindle speed 5000rpm, feed 1.8mm/min and 100min. To check the feasibility of process for metallic workpiece a curve stainless steel workpiece of 6x6x0.8 mm with 4mm radius curvature was used. The final roughness achieved was Ra 0.005nm from Ra 230nm initial with parameter C-axis angular position 70⁰, spindle speed 5000rpm, feed 4.8mm/min and 300min. Aluminum oxide abrasive was used for the metallic workpiece because cerium oxide abrasive is not suitable for the stainless steel

2.2 Research Gap

From literature review, it has been observed that very less work done on the cylindrical surfaces. There is no present magnetorheological finishing (MRF) processes which can finish external cylindrical surfaces of ductile ferromagnetic material. Magnetic abrasive finishing (MAF) is only the process which used to finish the circular rods or shafts. But MAF are used only to finish the hard materials. If finishing is done on the soft material with MAF, the abrasive particles are embedded in the work-piece. Second it only finishes the single diameter shafts, stepped or grooved shaft cannot finish with this process. To overcome these problems the newly developed magnetorheological process as similar to turning operation needs to be explored further.

2.3 Objective of the Present Work

To achieve the main objective such as uniform magnetic flux density at tip of turning type magnetorheological finishing tool , the following sub-objectives are:

- To study the distribution of magnetic flux density at the tool tip surface with workpiece using MAXWELL ANSOFT V13 software (student version).
- To fabricate of turning type MRF tool with curve tip surface as similar to cylindrical surface with control magnetic field.
- To compare the performance of curve tip type tool with flat tip type tool.
- To check ability of curve tip tool perform experiments with various parameters (help of design of experiments) on cylindrical workpieces and measures the change in roughness.

2.4 Methodology

The current work is to achieve the uniform magnetic flux density at MRF the tool tip surface. The step by step methodology has been defined for the development of turning type MRF setup.

- Prepare CAD model of curve tip type MRF tool.
- Finite element (FE) analysis of new MRF tool using MAXWELL ANSOFT V13 (student version) to study the magnetic flux density.
- Fabricate the tool according to the design.
- Check performance of the curve tip type tool and compare results with the flat tip type tool.
- Perform experiments with various parameters with help of design of experiments on cylindrical workpieces and measures the change in roughness.
- Optimize the parameters for the particular workpiece material for best results.

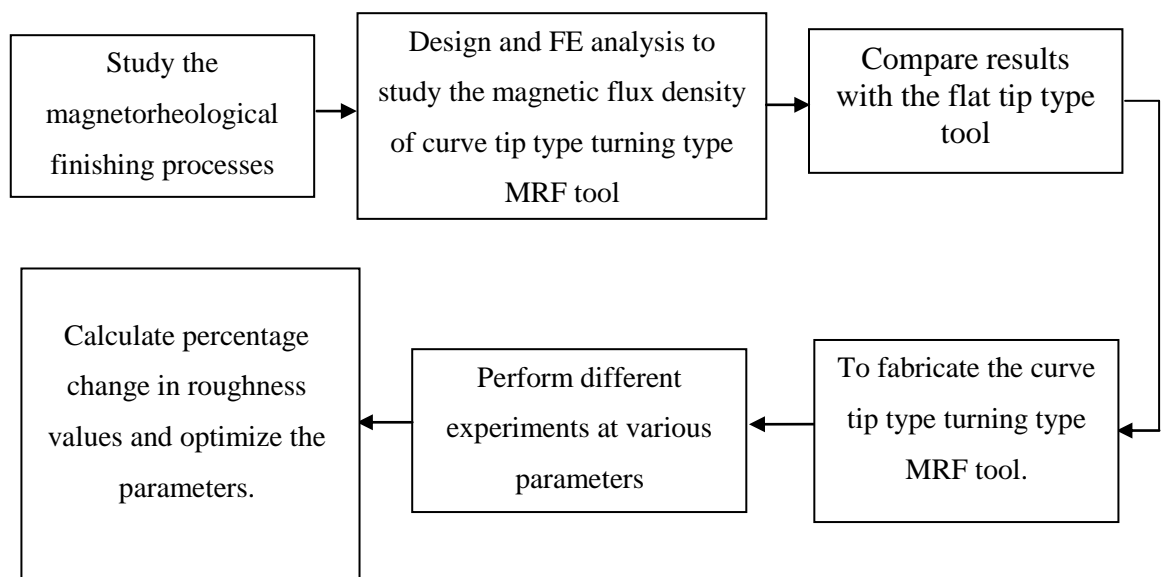


Figure 2.3: Flow diagram of methodology steps followed for completing the present objectives

Chapter 3

Magnetorheological Finishing Process for External Cylindrical Workpieces with Turning Type Tool

The process is recently developed for finishing the cylindrical components. The setup used is similar to a lathe machine with some modifications in the BEMRF process. The ordinary BEMRF tool has a rotatable core whereas in the turning type tool the core remains stationary and the rotational motion is given to the workpiece as similar to the turning operation. Due to the periphery of the cylindrical surface the tool tip has been modified to same curvature as that of the cylindrical workpiece. This tool tip is detachable and can be replaced with a different tip as per the requirement of external cylindrical surfaces. The modified BEMRF tool is referred as turning type MRF tool. This setup is similar as lathe machine, in this process instead of single point turning tool the magnetorheological tool is used to finish the cylindrical external surface. The workpiece and tool tip are not contact with each other and the finishing is done with the help of MRF fluid. The workpiece is fixed in the chuck and rotated; gap is maintained between the tool and workpiece. The MRF fluid is between the maintained gap and remove the material from the workpiece in micro chips. The process is used to finish the external type of cylindrical surfaces such as groove, step surfaces and threads.

3.1 Turning Type Magnetorheological Finishing (MRF) Process

The schematic representation of the present turning type magnetorheological finishing process is shown in Fig 3.1.

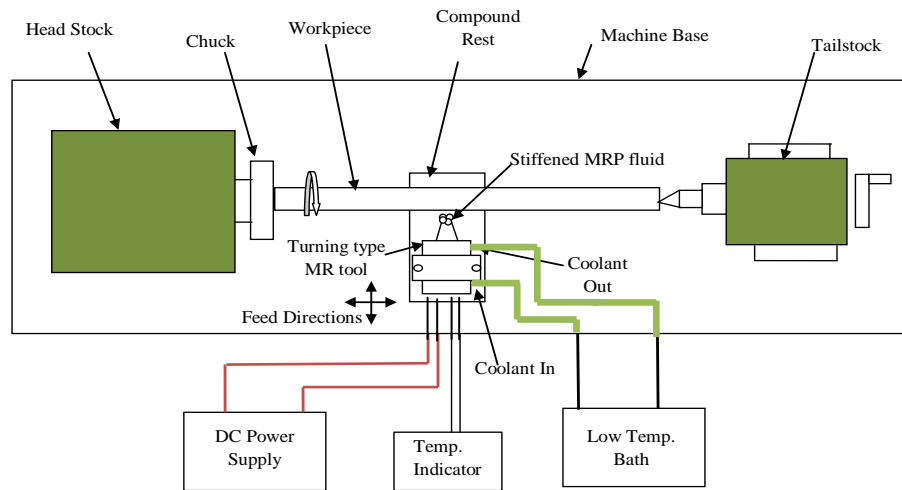


Figure 3.1: Schematic diagram of turning type MRF experimental setup

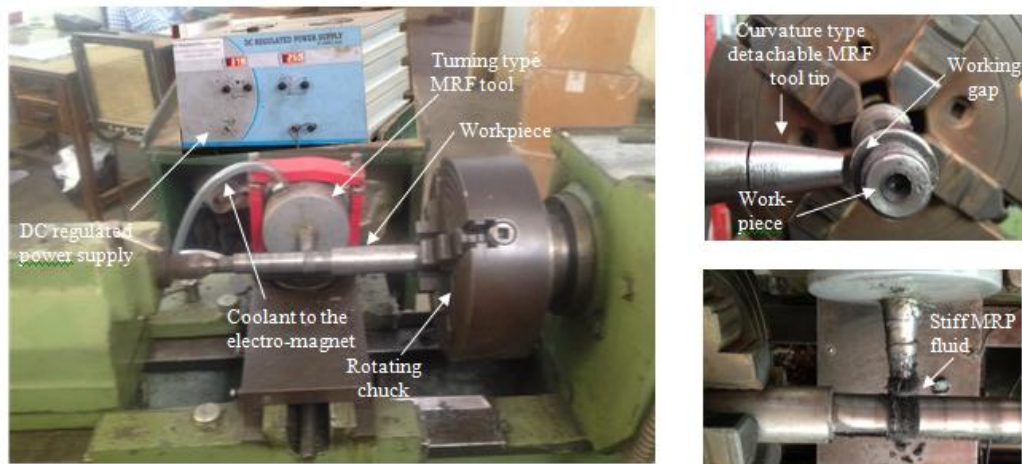


Figure 3.2: Photograph of turning type MRF experimental setup

In MRF processes the magnetic field is controlled by controlling the DC supply to the electro magnet. The viscosity of MRP fluid is increased by increasing the current, more fluid viscosity results in more shear force which help for material removal. More the magnetic field density CIP's attracts towards the tool tip and makes the strong chains which hold the abrasive strongly and responsible for finishing [Singh *et al.*, 2011].

3.1.1 Mechanism of Material Removal

There is relative motion between the workpiece and the turning type magnetorheological tool so that the material removal in this process is due to abrasive action. There are three forces (axial, normal and cutting force) responsible for the material removal. Normal magnetic force is responsible for indentation of abrasive particles in the workpiece, axial and cutting force is responsible to remove the material from the workpiece in the form of microchips. When the MRP fluid is applied on the tool tip and switched on the electromagnet the CIP's makes chains and hold the abrasive particle between the chains and provide strength to remove the material. Abrasives between the CIP's chains act as a multi cutting tool. The mechanism of material removal in turning type magnetorheological finishing process is shown in Fig 3.3.

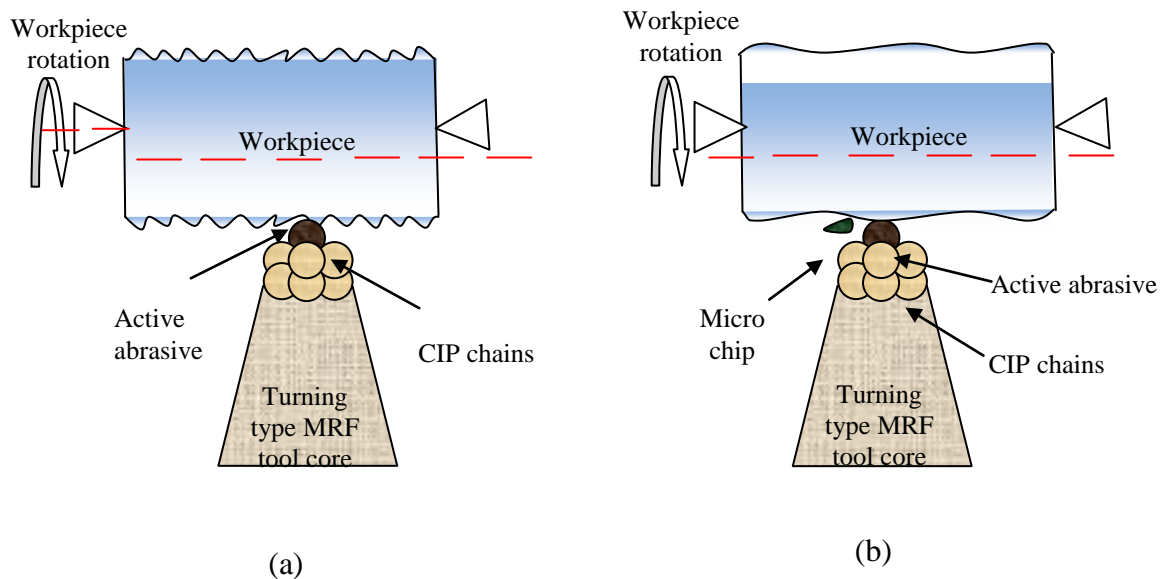


Figure 3.3: Schematic diagram of mechanism of material removal (a) initial surface roughness peaks of workpiece and gripped abrasive with CIPs (b) Chip removal in finishing

3.2 Finite Element Analysis of the Present Turning Type MRF Tool

MAXWEL ANSOFT V13 (student version) software is used to do the finite element analysis of the present MRF turning type tool and simulate the magnetic flux density. The finite element analysis helps to determine the magnetic field density at the tool tip and workpiece. Various steps are used in MAXWEL ANSOFT V13 (student version) for finite element analysis. The steps used in this analysis are as follows:-

At starting of the finite element analysis, firstly make a model of electromagnet according to design with or without workpiece in MAXWEL ANSOFT V13 (student version). When the model is completed, the material assigned to the different components of the tool. The MRP fluid is also filling in gap between the workpiece and tool tip. Relative permeability assign to this MRP fluid is 5. After this the boundaries and constrains has been selected i.e. insulating the copper coil, slave, master etc. Excitations are selected to execute the analysis. In excitations there are different parameters i.e. current, voltage, current density etc. to calculate the force, torque, magnetic field density and matrix. In last step before analysis validate the model first and then add solution setup and assign analysis. In this step magnetic fields B (tesla) is drawn at proper plane to analysis magnetic field intensity. Boundary conditions for finite element analysis are working gap, current and number of turns of copper coil. In present analysis we keep current 3Amp, number of turns 2800 and varying the working gap from 0.5 to 2.5 in five steps.

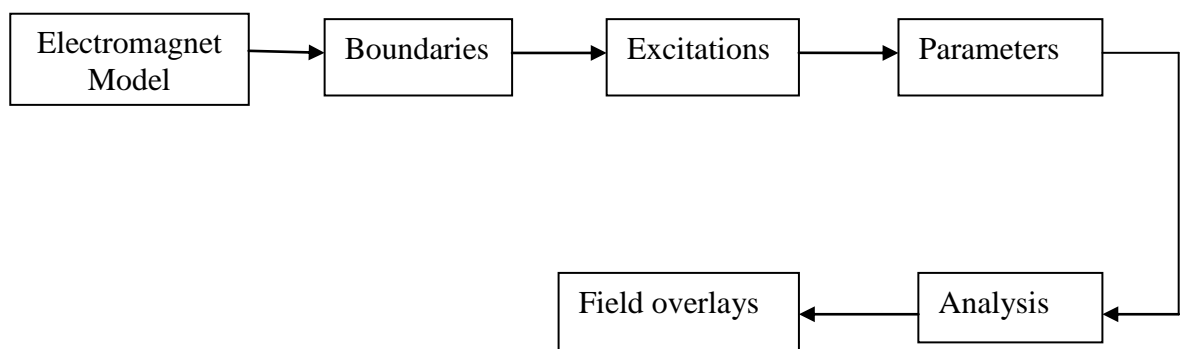


Figure 3.4: Flow chart of different phases in Maxwell ansoft V13 for analysis of magnetic flux density

Table 3.1 shows the parameters, material and material relative permeability which are assigned to the different components of the tool and workpiece. The magnetic simulation results are performed to analyze the magnetic flux density distributions on the assigned data with varying working gap between the tool tip and the workpiece. The electromagnet model of flat tip surface of with external surface of cylindrical workpiece MRF tool is shown in Fig 3.5.

Table 3.1: Assigned parameters with material and relative permeability to electromagnet model

| Parameter | Material | Relative permeability | Current | No. of turns |
|--------------------|-----------|-----------------------|---------|--------------|
| Electromagnet coil | Copper | 0.999999 | 3A | 2200 |
| Solid core | Iron | 4000 | | |
| MR polishing fluid | MRP fluid | 5 | | |
| Workpiece | Iron | 1500 | | |

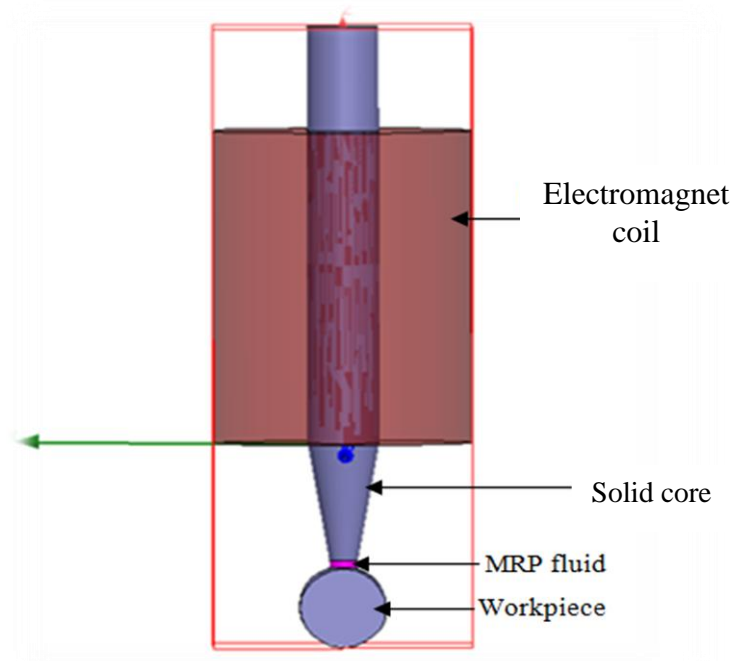


Figure 3.5: Electromagnet model of turning type MRF flat tool tip with external cylindrical surface

3.3 Comparison Between MRF Tool with Flat Tip Surface and Curve Tip Surface

The simulation results of flat tip type tool with the help of MAXWELL ANSOFT V13 (student version) shown the magnetic flux density at flat tool tip at different working gap between the tool and workpiece. Fig.3.6. show the magnetic flux density at various working gaps. Fig.3.6.(a) shown variation of magnetic flux density at tool tip when the working gap is 0.5 mm. It is clear the magnetic flux density is not uniform across the tool tip surface, this is because of the gap is not uniform between the workpiece and tool tip surfaces due to flat tool tip with cylindrical surface. The magnetic flux density is maximum at the centre of tool tip surface and decreased when move away from the center. Because of maximum magnetic field intensity at the tool tip the CIP's and abrasive particles make the finishing brush on the tool core tip which helps to finishing the workpiece. Due to non uniform working gap, the CIP's chains are very stronger at the center of tool tip as compared to its corners. This results in not uniform finishing. Magnetic flux density value on flat tip type tool with different working gap is reported in Table 3.2.

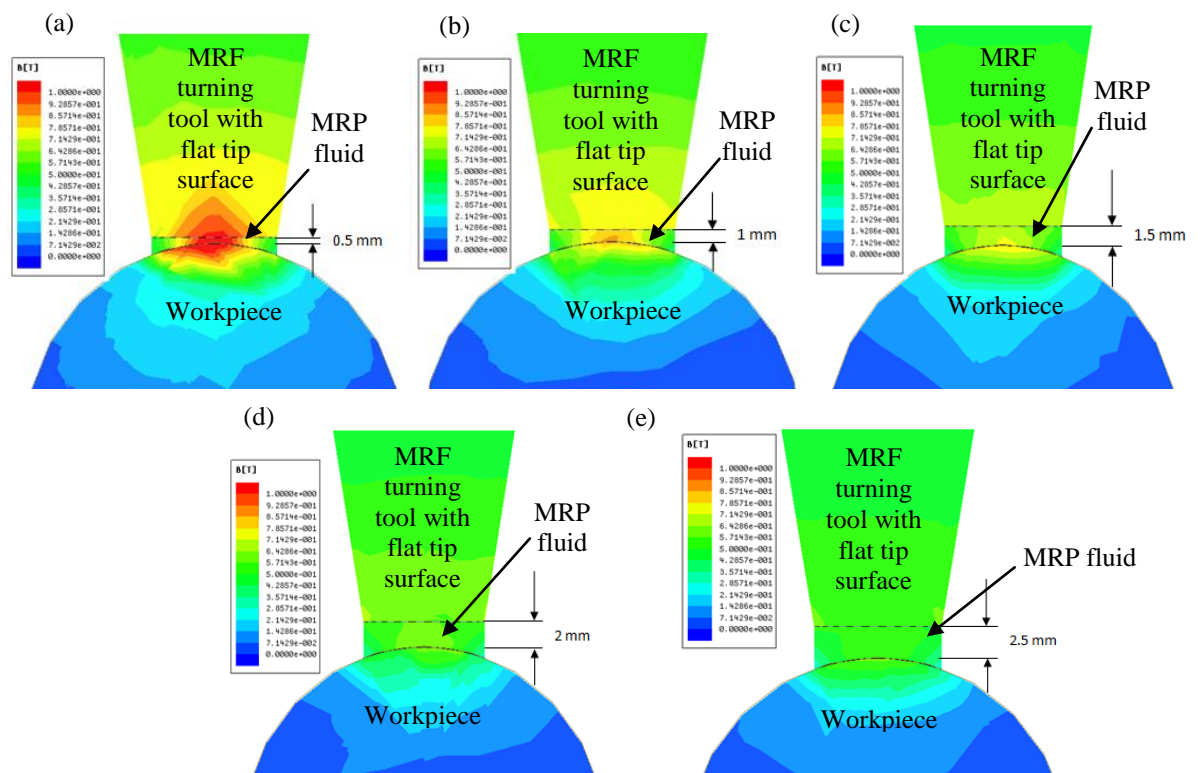


Figure 3.6: The magnetic flux density distributions at flat type tool tip at different working gap

Table 3.2: Magnetic flux density with flat tool tip at different working gaps in Tesla

| S. No | Working Gap In mm | Magnetic flux density B (T) |
|-------|----------------------|-----------------------------|
| 1 | 0.5 | 1 |
| 2 | 1 | 0.7857 |
| 3 | 1.5 | 0.7142 |
| 4 | 2 | 0.6428 |
| 5 | 2.5 | 0.5714 |

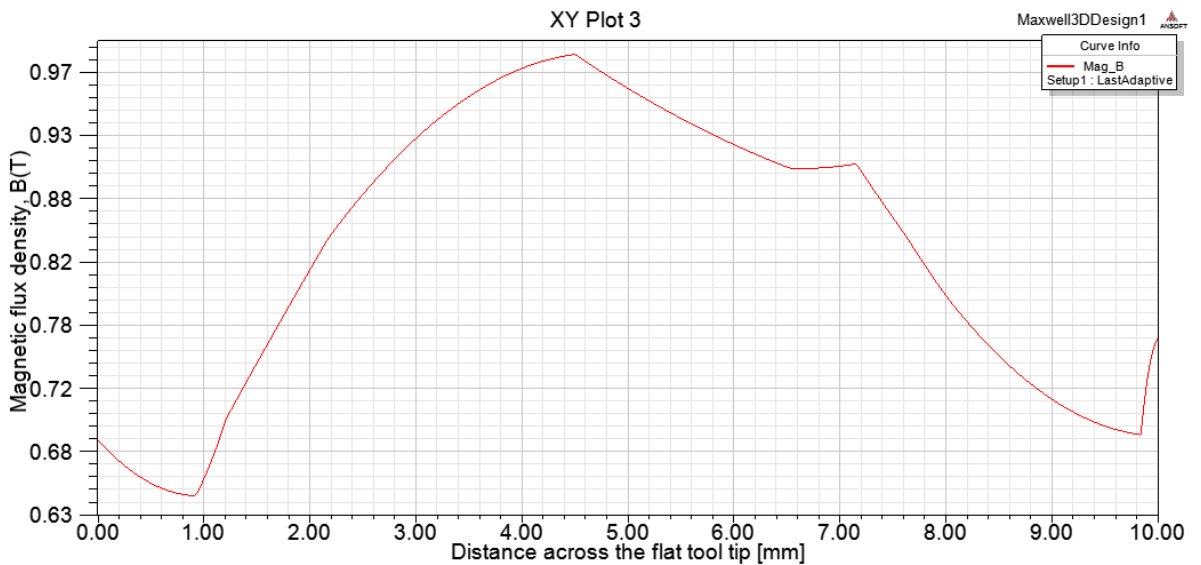


Figure 3.7: Magnetic field density distribution at distance across the flat tool tip surface

To achieve the uniform magnetic flux density the tool tip is modified. In modified tool tip, the tip is made with similar curve of workpiece diameter on tip of tool. Because of similar curve, the gap between workpiece and tool tip was uniformed. With MAXWELL ANSOFT V13 (student version), it also see that there is no variation in magnetic field density along the tool tip which is almost uniform on curvature. Uniform magnetic field density helps to form the uniform chains at the tool tip, the strength of chains is easily controlled by regulating the DC supply. Because of uniform magnetic flux density the curve tool tip can perform better than the flat tool tip. Figure 3.8 show the magnetic flux density variation along the tip of new curve type tool. It is clear that magnetic flux density is almost uniform all over tool tip. The magnetic field density in curve tip type tool is uniform but less effective than the flat

tip type tool under same conditions. Magnetic field density at curve tip type tool is reduce due to many reason like there is some air gap between the tool tip attachment and tool core, because of material loss at the end of tip or shape of magnet also effect on the magnetic field density. Magnetic flux density value on curve tip type tool with different-2 working gap is showing in Table 3.3.

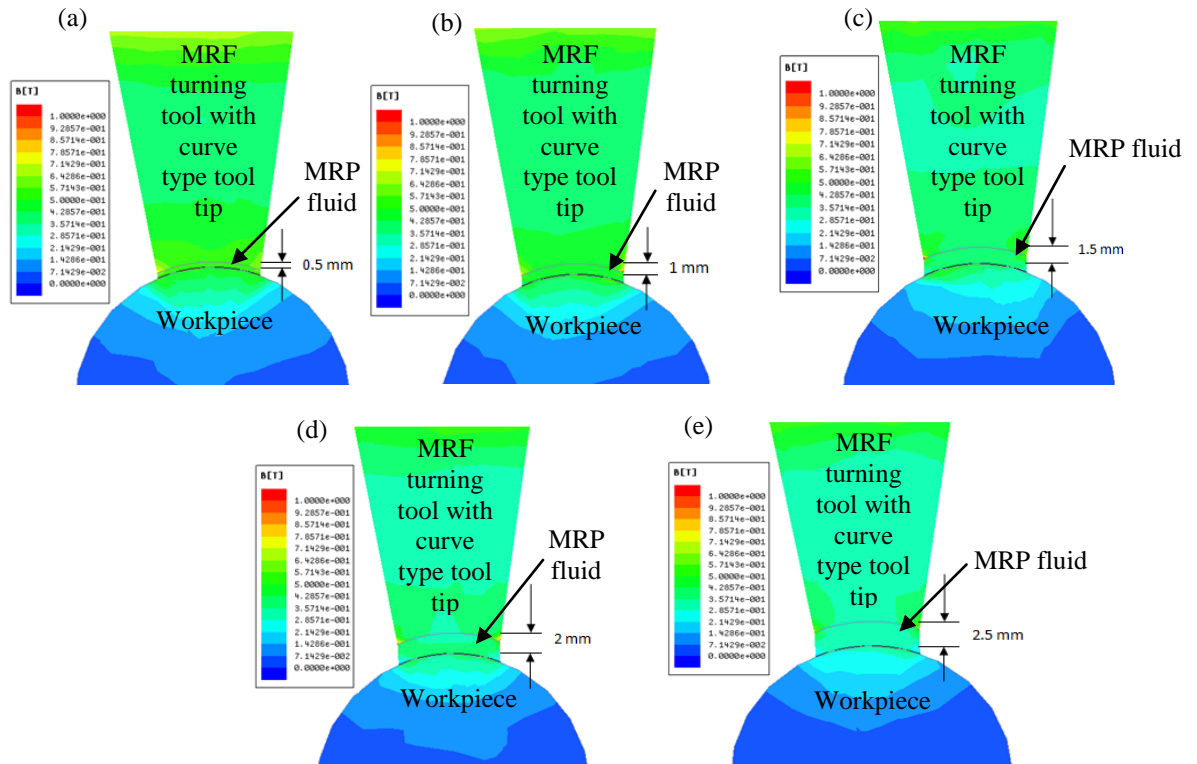


Figure 3.8: Magnetic flux density distribution at curve type tool tip at different working gap

Table 3.3: Magnetic flux density with curve tool tip at different working gaps in Tesla

| S. No | Working Gap Z (mm) | Magnetic flux density B_z (T) |
|-------|-----------------------|---------------------------------|
| 1 | 0.5 | 0.7142 |
| 2 | 1 | 0.6428 |
| 3 | 1.5 | 0.5000 |
| 4 | 2 | 0.4285 |
| 5 | 2.5 | 0.3571 |

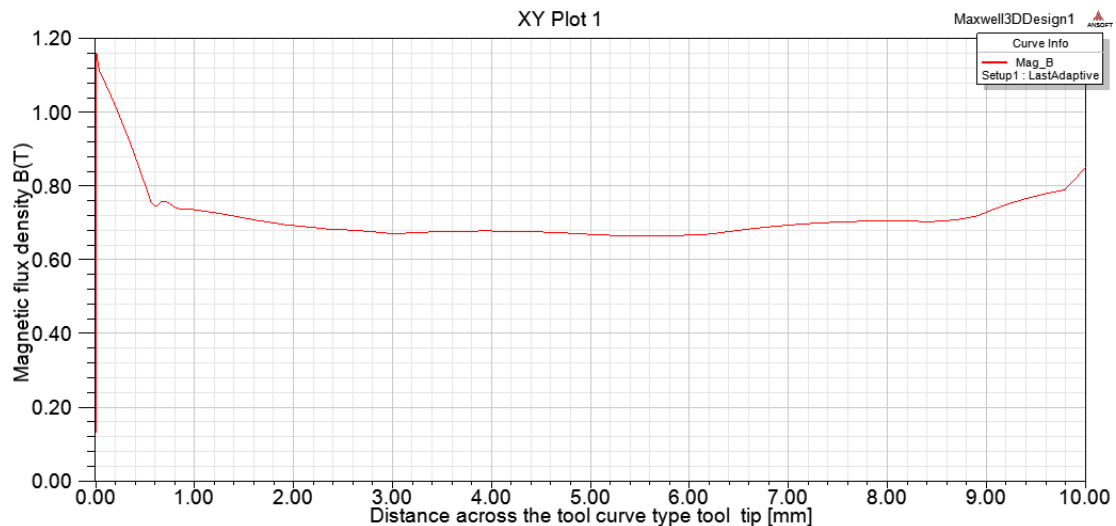


Figure 3.9: Magnetic field density distribution at distance across the curve tool tip surface

Fig. 3.7 and 3.9 shows the magnetic field density at the both type of tool tips from one corner to other corner of tip. Clearly seen from both figures, the magnetic field density is more uniform on the curve type tool tip than the flat tool tip. The variation in the magnetic field density is very less in curve type tool tip. In flat tool tip surface the magnetic field density is very less as compared to the center of the tool tip.

It is observed from the magnetic simulation that the strength of the magnetic flux density is depended upon electric current and working gap. Strength of the MRP fluid is controlled by controlling the electric current to the electromagnet coil. It is observed that the working gap between the tool tip and the workpiece surface is an important parameter for the strength of the finishing spot. It is observed that at the same electric current value by varying working gap the strength of the magnetic field changes. If working gap is minimum the MRP fluid become more stiffen as compare to higher working gap at the same electric current. Magnetic simulations are conducted at the working range from 0 mm to 2.5 mm. Using all these information obtained from the magnetic simulation, the further design of MR finishing tool has been preceded for generating uniform and maximum magnetic flux density at the tool tip surface.

3.3.1 Comparison Between MRF Tool with Flat Tip Surface and Curve Tip Surface (experimentally)

The best condition captured from the experimental range of the variable was $N= 443$ rpm, $I= 2$ A and $Z= 0.5$ mm when the experiments was performed with flat tool tip type magnetorheological turning type tool. The surface roughness obtained after finishing at these conditions 310 nm from the initial roughness value 680 nm after 90 minutes of finishing time.

To check the curve tip type tool performance, the experiment was performed with same parameters; $N= 443$ rpm, $I= 2$ A and $Z= 0.5$ mm. The significant change in roughness was observed at same conditions with the curve tip type tool. The surface roughness was decreased from 680 nm to 130 nm with new curve type tip tool after same finishing time.

From this practical experimental result it was conformed that the curve type tip tool is better finishing performance than the flat tip type tool.

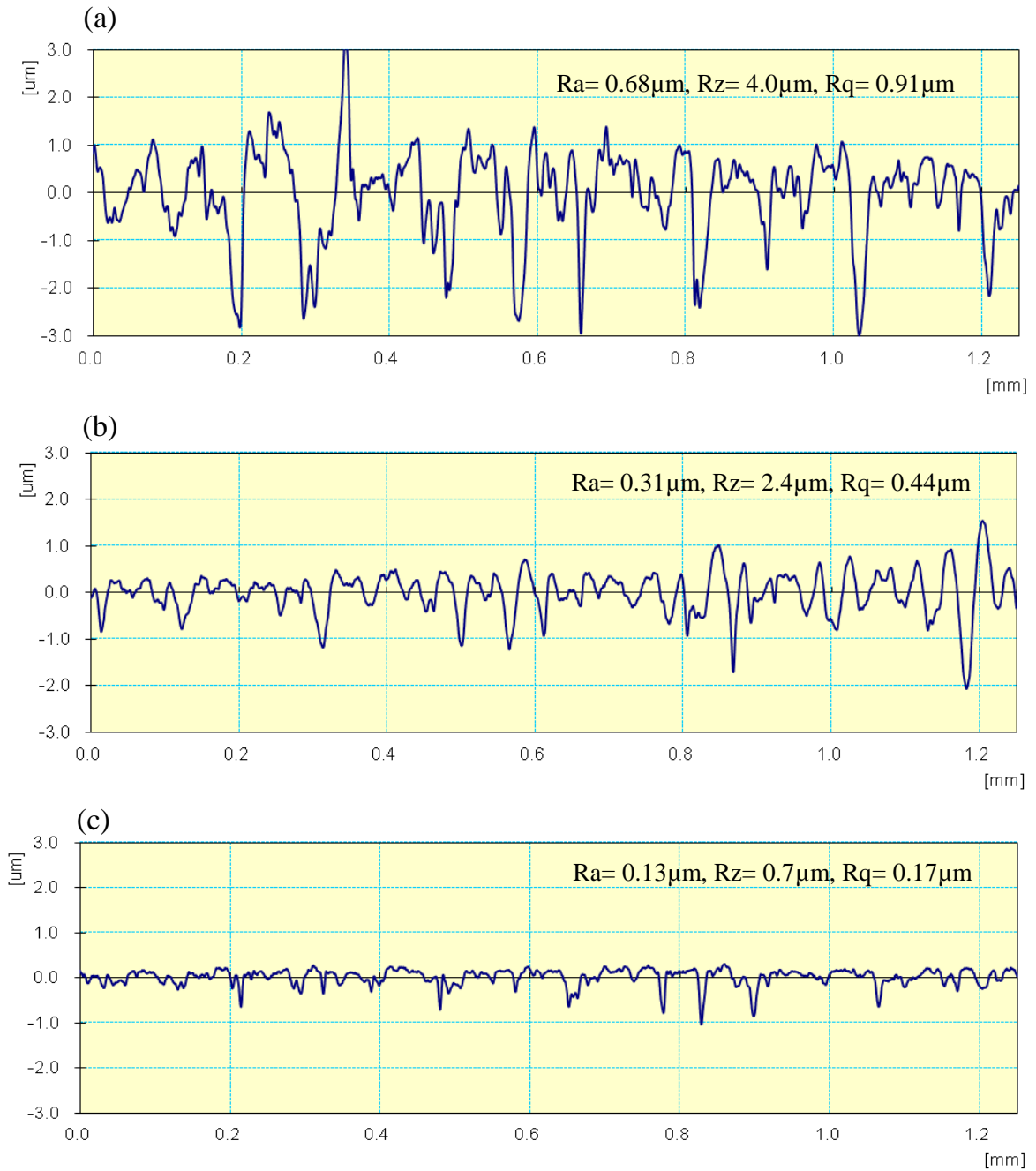


Figure 3.10: Surface roughness profiles (a) initial, (b) flat tool tip surface and (c) curve tool tip surface after 90 minutes of finishing on external surface of cylindrical mild steel workpiece at rotational speed of 443 rpm, electromagnet current of 2A and working gap of 0.5 mm

3.4 Lathe Machine Specifications

Lathe is a machine tool which rotates the workpiece at its central axis to perform various operations. The MRF tool which is applied to the workpiece is symmetric about the axis of rotation. The turning type MRF tool used to finish external cylindrical objects. The MRF tool is attached at the lathe machine for finishing the external cylindrical object. The present lathe machine where experimental setup has been build up technical specifications are listed in table 3.4.

Table 3.4: Technical specification of the present lathe machine

| | |
|----------------------------|---------------|
| Model | 1050/1 |
| Height of centers | 175mm |
| swing over bed | 335mm |
| Swing over saddle | 230mm |
| Distance between centers | 800mm |
| Bed | |
| Bed type | 2 flat & 2v |
| Bed width | 254mm |
| Main spindle | |
| Spindle bore | 42mm |
| Tail stock | |
| Spindle diameter | 45mm |
| Tool slide | |
| Travel of tool slide | 140mm |
| Speeds | |
| No. of speeds | 8 |
| Range RPM | 45-938 |
| Electrical | |
| Main motor | 2HP/1440rpm |
| Other data | |
| Weight | 800kgs |
| Floor space occupied (L*W) | 1700*940 |

3.5 CAD Model of Turning Type MRF Tool

Components used to make the turning type MRF tool

- Mild steel solid core
- Bakelite supports for coiling
- Copper wire
- Snap ring
- PVC casing
- Thermocouple
- Inlet and Outlet ports for cooling fluid

To make a electromagnet, the required core material should have the good magnetic property. Therefore mild steel is selected to make the solid core of tool. Two Bakelite supports are used with the core to hold the winding at proper position. The Bakelite supports are hold with help of snap rings (circlips). The material used for the coil is 20 gauge copper wire having relative permeability 0.99999 and the material is used for the inner core having relative permeability 4000. The relative permeability of the MRP fluid is assigned as 5. Transformer oil is used to cool the copper winding. The transformer oil is circulate with the help of low temperature bath and keeps in directly contact with copper winding that is inside the cooling jacket which is made of PVC material. A thin film type RTD (resistive temperature device) temperature sensor is also placed in the winding near the core to measure the temperature of tool core as well as electromagnet. Temperature of core should not increase more than the 50 °C-60 °C otherwise MRP fluid properties can be changed which affects the finishing. The CAD model of MRF tool and drawing of each part are shown in Fig. 3.11 and Fig. 3.12 respectively.

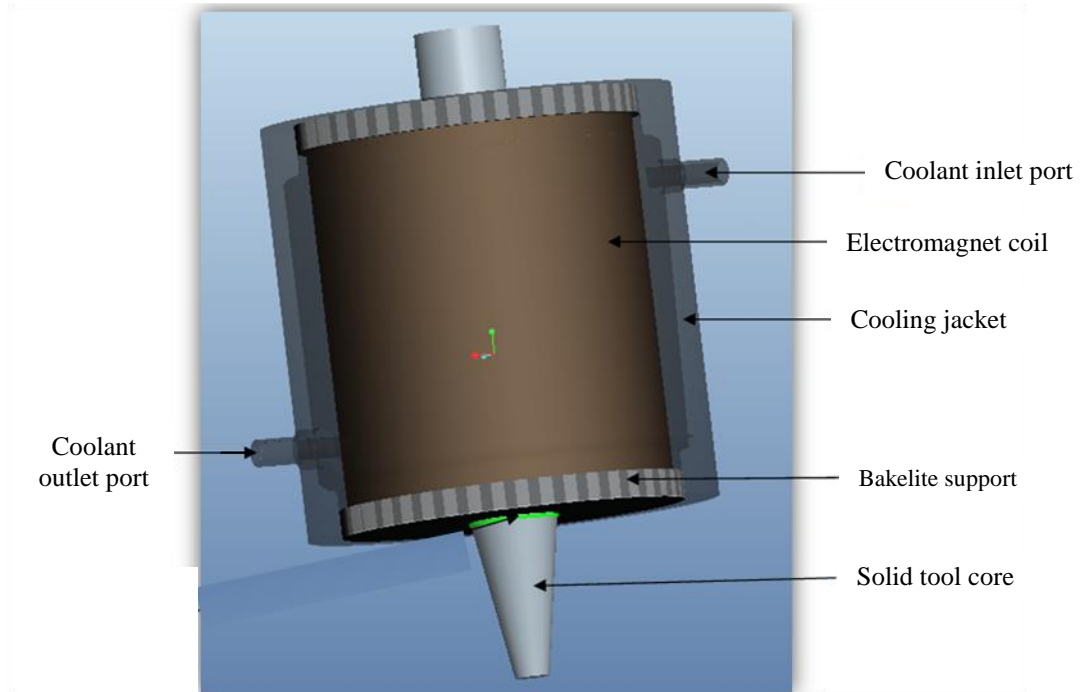


Figure 3.11: 3D CAD model of MRF tool

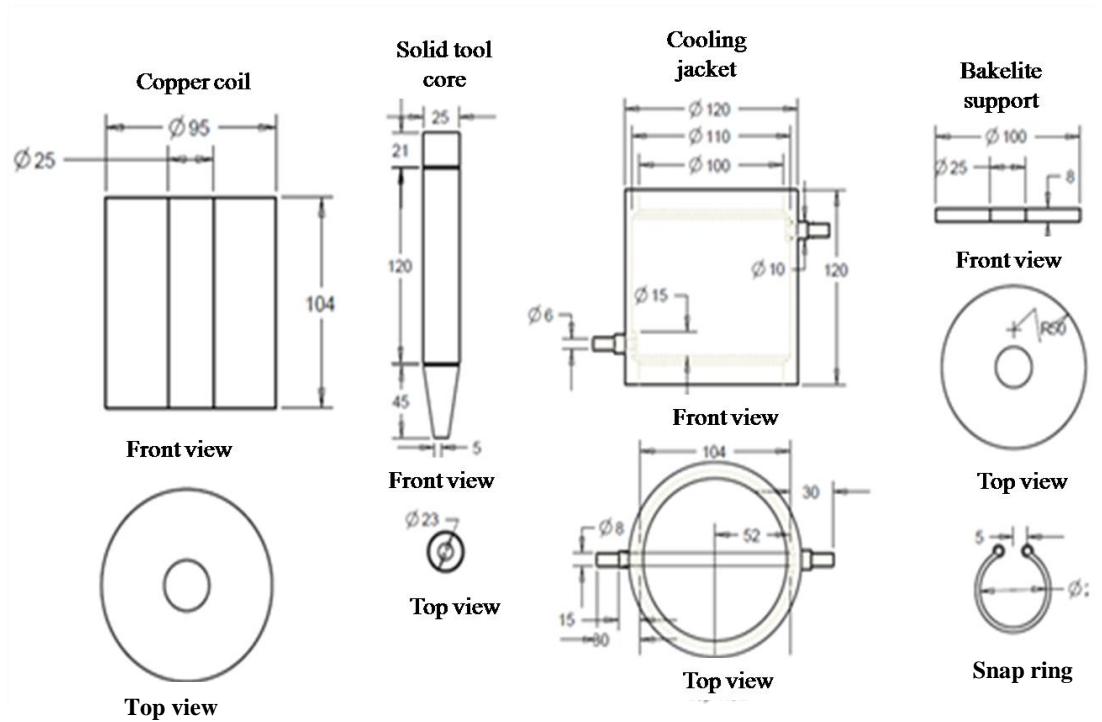


Figure 3.12: Drawings of MRF tool parts

3.6 Stirring Machine to Mixing the MRP Fluid

The purpose of stirring machine is to mix the constituents of MRP fluid. In MRF process, use a mixture of carbonyls iron powder, abrasive and base fluid. This fluid is of very high viscosity and to obtain the desired result, required to mix these constituents of MRP fluid properly and thoroughly. Due to viscosity of MRP fluid an apparatus is required which is powerful and rugged enough to thoroughly mix the constituents of MRP fluid. The mixing time is generally not more than 1 hour. So, a stirring machine has been fabricated which facilitates the required purpose. The CAD model and photograph of stirring machine is shown in Fig. 3.13 & 3.14.

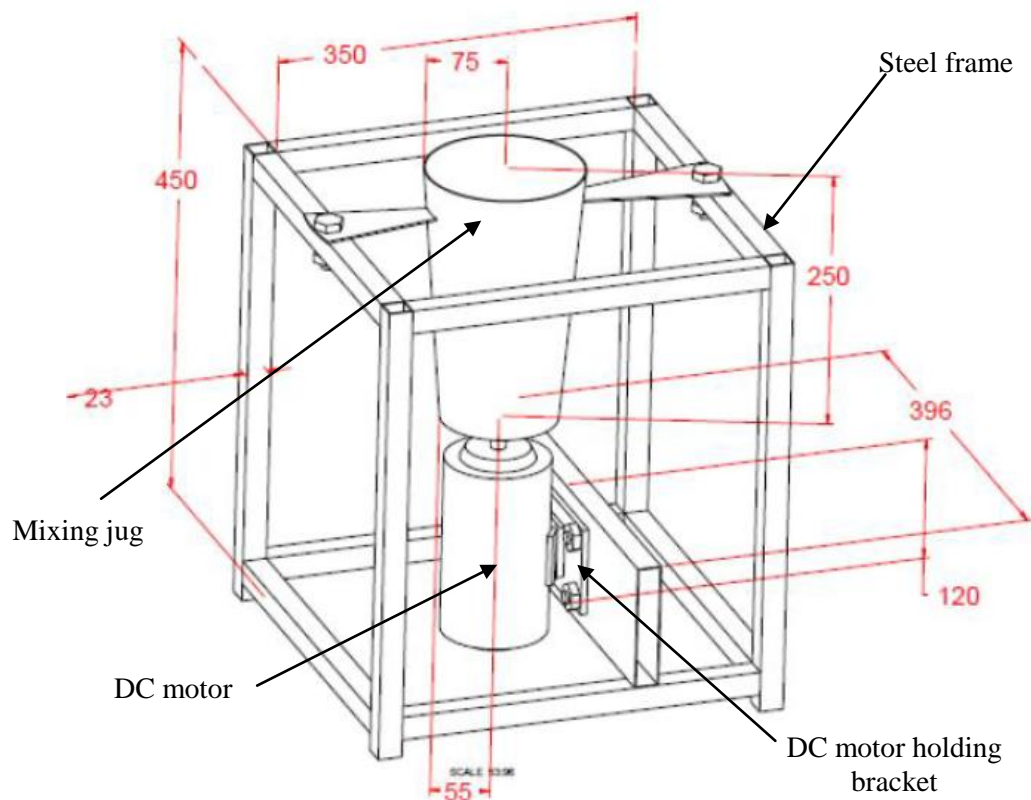


Figure 3.13: CAD model of stirring machine

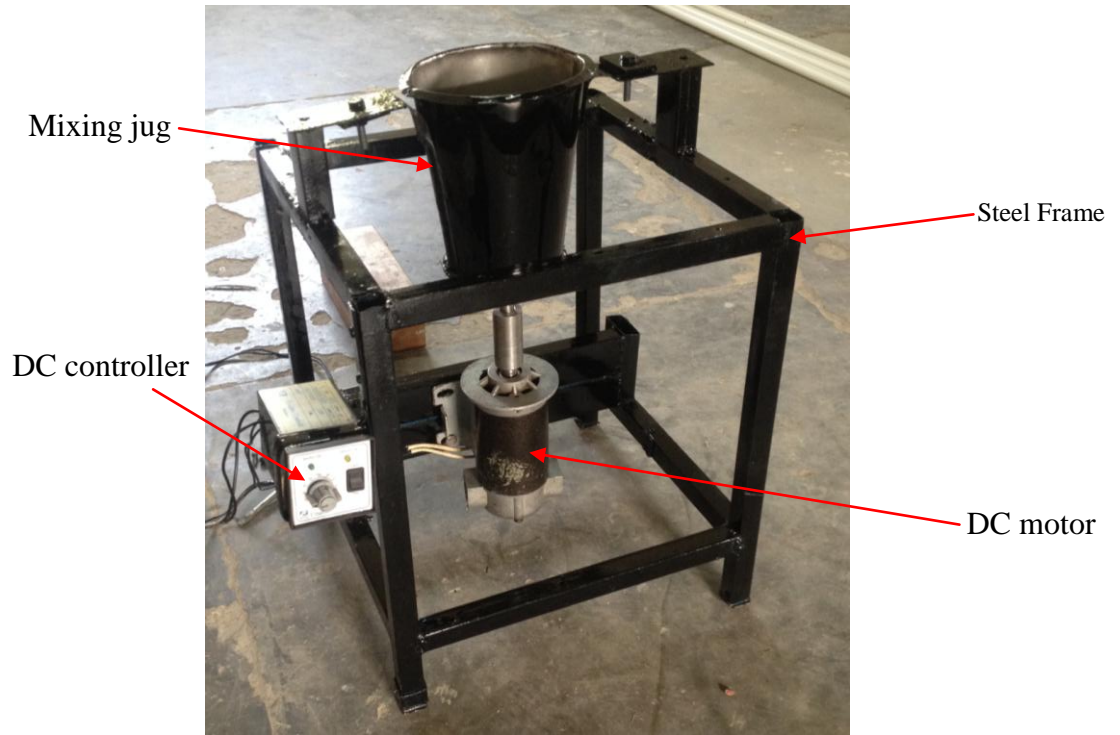


Figure 3.14: Photograph of MRP fluid stirring machine

3.7 Preliminary Experiments on Permanent Mould Punch Die with Curve Tool Tip Surface of MRF Turning Type Tool

For experimentation the workpiece is choose from practical application. It is a die punch which is used to make the syrup measuring caps. The material of workpiece is P20 a type of die steel as it is ferromagnetic in nature. Very fine finishing is required on the outer surface of workpiece to achieve the better surface on the casting product.

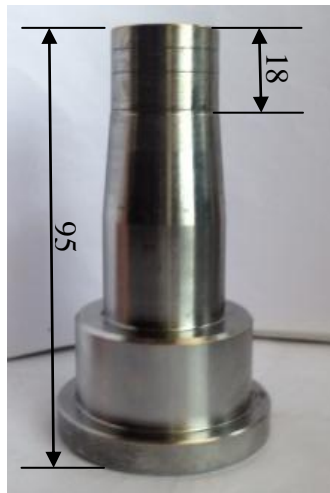


Figure 3.15: Photograph of permanent mould die punch

Before start experimentation, checked the initial roughness of the workpiece on the surface roughness tester and mirror image test. Surface roughness test is done with cut of length 0.25 mm. The initial surface readings were $R_a = 0.53\mu\text{m}$, $R_z = 2.6\mu\text{m}$ and $R_q = 0.63\mu\text{m}$.

3.7.1 Parameters and Conditions

Experimentation was done with parameters magnetizing current= 2 A, working gap= 0.6 mm and rotational speed= 284 RPM.

The MRP fluid used for finishing was prepared with composition of 20% CIP's, 20% Sic abrasive and 60% base fluid (80% paraffin wax and 20% AP3 grease).

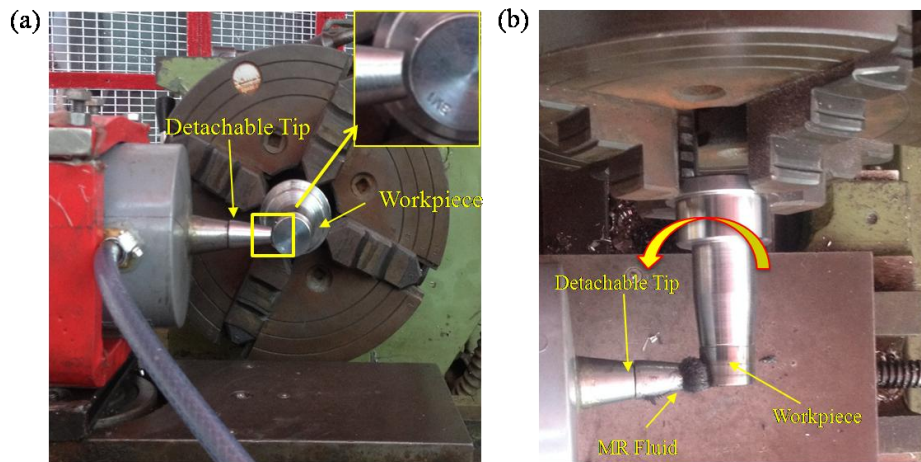


Figure 3.16: a) Front view of the workpiece held in a four jaw chuck and gap maintained between the detachable tool tip and cylindrical surface of the workpiece, (b) top view of the workpiece with MRP fluid filling the gap between tool tip and cylindrical surface during the finishing process

3.7.2 Result

The finishing was done for 120 minutes, the surface roughness was significantly decreases from $R_a= 0.53\mu\text{m}$, $R_z=2.6\mu\text{m}$ and $R_q= 0.63\mu\text{m}$ to $R_a= 0.08 \mu\text{m}$, $R_z= 0.7 \mu\text{m}$ and $R_q= 0.14\mu\text{m}$. The surface roughness profiles and mirror images of initial and after finishing is shown in Fig. 3.17 & 3.18.

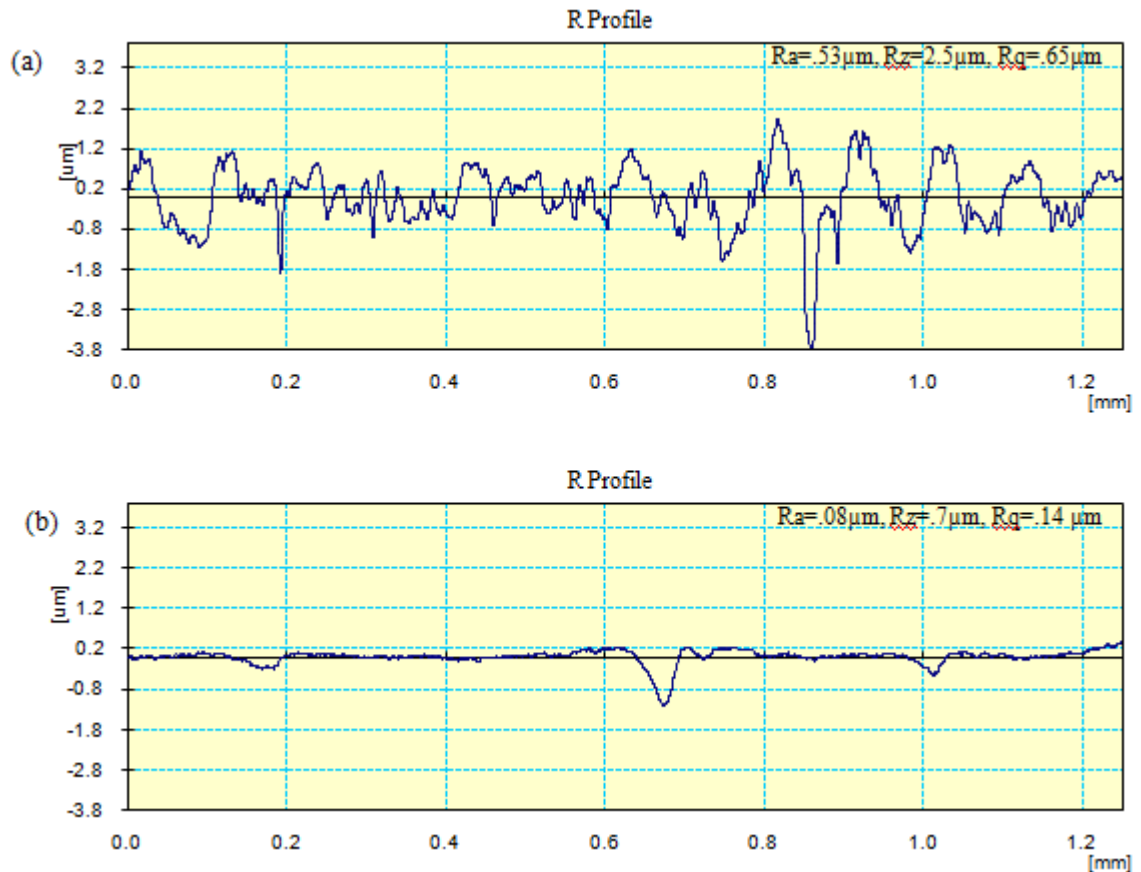


Figure 3.17: Roughness profiles of cylindrical surface of the permanent mould punch
(a) before and (b) after 120 minutes of finishing

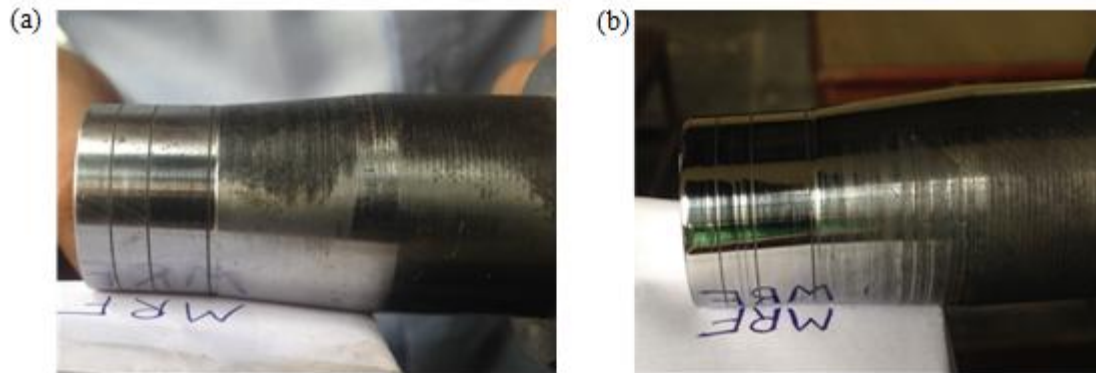


Figure 3.18: Mirror image of cylindrical surface of permanent mould punch (a) before and (b) after 120 minutes of finishing

Surface roughness profiles and mirror images demonstrated significant enhancement in surface quality of finished surface of permanent mould punch as compared to its initial surfaces. The turning type magnetorheological finishing processes were demonstrated its capability for finishing of permanent mould punch.

3.8 Conclusion

From, the comparison of curve tip type tool and flat tip tool and preliminary experiments the following conclusion was concluded.

- The magnetic simulation shows the magnetic flux density on the tool tip, which shows the magnetic flux density, is more uniform on the curve type tip tool than the flat tip tool.
- The surface roughness was reduce to 130 nm from initial surface roughness 680 with curve tip tool and from 310 nm from initial surface roughness 680 nm with flat tip tool when the finishing done at workpiece rotation speed 443 rpm, current 2A and working gap 0.5mm.
- Permanent mould punch was finished with curve tool tip turning type magnetorheological finishing process. The surface roughness value was reduced from 530 nm to 80 nm in 120 min at magnetizing current 2A, working gap 0.6 mm and rotational speed 284 rpm.

Chapter-4

Synthesis of MR Polishing Fluid and Experimentation

To study the performance of improved turning type MRF tool, the plan of experiments were performed on ferromagnetic mild steel work-piece surface for studying the % reduction in surface roughness values.

4.1 Preparation of MRP Fluid

The MR polishing fluids have been prepared indigenously and used as finishing medium for the experiments. MRP fluid is prepared with combination of 20 volume % of carbonyl iron particles, 20 volume % of abrasive particles (silicon carbide powder) and 60 volume % of base fluid (80 wt % of heavy paraffin oil and 20 wt% of AP3 grease) [Singh *et al.*, 2011] start with mixing the heavy paraffin oil and AP3 grease in stainless steel funnel with multi blade stirrer which is controlled by DC RPM controller on DC motor. Mix abrasives and carbonyl iron particles for some time and add into the base fluid. The mixing is done with very slow to avoid the sedimentation of carbonyl iron particles at the bottom of the mixing funnel.

4.1.1 Preparation of base fluid

In the composition of 1 kg (1000 grams) base fluid, heavy paraffin oil is 80% by weight= 800 gram And AP3 grease is 20% by weight= 200 gram. For preparing the base fluid stirrer heavy paraffin oil for some time and added AP3 grease slowly into it. Keep stirring for sometime till both paraffin oil and grease mixed properly in each other. For density measurement, a sample was taken of base fluid of 20 cm³ and weighted it.

Density = mass per unit volume.

Therefore, the density of base fluid=0.76 gm/cm³

4.1.2 MR Polishing Fluid

Total sample of MRP-fluid was prepared as 0.4 l=400 cm³. Composition is CIP is 20% by volume =80 cm³ and by weight= 80 cm³×7.8 gm/cm³ (density of CIP) =624 gm/cm³=0.624 kg. The silicon carbide abrasive powder is 20% by volume=80 cm³ and by weight=80 cm³×3.22 gm/cm³ (density of silicon carbide abrasive powder) =257.6 gm. The base fluid is 60% by volume=400 cm³×60%=240 cm³ and by weight=240 cm³×0.76 gm/cm³ (density of base fluid) = 182.4 gm/cm³.

The above mention MRP-fluid was mixed and stirred in funnel. The % volume concentration of Constituent to prepare MRP fluid is shown in table 4.1 below.

Table 4.1: Composition of MR polishing fluid

| Constituent | % Volume concentration |
|---------------------------------------|------------------------|
| Base fluid medium | 60 |
| Silicon carbide | 20 |
| Carbonyl iron powder of mesh size 800 | 20 |

4.2 Turning Type MRF Process Variables

Turning type MRF process is a new finishing process for cylindrical external surfaces so lack of data is available in literature.

4.2.1 Rotational Speed of the Workpiece (N)

Rotating speed of the workpiece effects the finishing of the work surface. The shear force is responsible for the material removal in form of micro chips during rotation of the work surface with the finishing spot of MRP fluid. Experiments are conducted from speed 150 to 750 rpm; obtain from the level of statistical design. The range was chosen on the basic of preliminary experiments.

4.2.2 Electromagnet Current (I)

The change in the rheological properties of turning type MRF process the finishing spot of the MRP- fluid at the tip mainly depends upon the magnetic flux density (supply of electric current in to the electromagnet coil). The finishing spot is also control by controlling the electric current. The bonding strength between the carbon iron particles is responsible for the material removal. The experiments are conducted from 0.5A to 4.5A.

4.2.3 Working Gap (Z)

Working gap is distance between the work-piece and the tip face of the MRF tool. The finishing spot at the tool tip face is controlled by changing the working gap keeping the electric current to be constant. It means that, for the better finishing spot at the work surface and to remove max peaks, the tip of the tool keep closer to the work surface at constant current supply. Similarly when the tool tip is make distance from the work-piece at the equal magnetizing current the finishing spot of the MRP fluid is less stiff. The experiments are conducted in a working range of 0.5mm to 2.5mm. These values are chosen from the simulation result as presented in chapter-3.

4.2.4 Abrasive Mesh Size (A)

Abrasives are the main constituent of MRP fluid. Mainly abrasives are the responsible for material removal and finishing. Fine abrasive can reduce more surface roughness than the coarse abrasive. The experiments conducted in a range of 400 mesh size to 1200 mesh size.

4.3 Design of Experiments

Designed experiments were used to examine the weight age of variables on the percentage change in roughness value. The experiment performed on the turning type MRF process setup as shown in Fig 3.2. Since the workpiece is in circular cross-sectional it is not easy to measure the surface morphology under a scanning electron microscopy (SEM), so to overcome this difficulties some small keys are cut in the workpiece of dimension 10x6x3 mm, which were option after grinding. The initial roughness was in range of 0.74 μm to 0.62 μm . the initial surface roughness is not the same for the every workpiece. The difference is taken by percentage change in the surface roughness value given by in Eq.4.1

The experimental setup is shown in Fig 3.2 in chapter 3. The workpiece is hold between the chuck and the dead centre on the lathe machine for the rotation, MRF tool attached at the carriage for the X-Y movement of the slides. The size of the tool tip diameter is 10mm and the workpiece length is same so that reciprocating motion in Y axis is not necessary during experimentation. The magnetizing current is switched on when MRP fluid is applied at the tool tip. A thick formation of MRP fluid formed at the tip surface. In full factorial experiments, the combination of factors represents the each experimental condition, and their response

is measured. To know the significance of regression equation ‘F’ test via analysis of variance (ANOVA) was conducted. The percentage change in the roughness value is measured. The initially material removal from experiments was too low; hence it is not consider as much response.

Table 4.2 shows the actual values in the turning type MRF process of ferromagnetic work-piece. The more experimental conditions are shown in Table 4.3. The turning type finishing process was conducted on ferromagnetic workpiece in arbitrary order, as per plan of experiments given in Table 4.4.

Table 4.2: Coded levels and corresponding actual values of the process parameters

| S. No. | Parameter | Unit | Levels | | | | |
|--------|-------------------------------------|-----------|--------|-----|-----|------|------|
| | | | -2 | -1 | 0 | 1 | 2 |
| 1 | Rotation speed of the workpiece (N) | RPM | 150 | 300 | 450 | 600 | 750 |
| 2 | Magnetizing current (I) | A | 0.5 | 1.5 | 2.5 | 3.5 | 4.5 |
| 3 | Working gap (Z) | Mm | 0.5 | 1 | 1.5 | 2 | 2.5 |
| 4 | Abrasive size (A) | mesh size | 400 | 600 | 800 | 1000 | 1200 |

From the Table 4.2 it is found that the speed of the workpiece varies from 150 rpm to 750 rpm, the electromagnet current is varied from 0.5A to 4.5A whereas the working gap is from 0.5mm to 2.5mm and abrasive size varies from 400 to 1200 mesh size.

Table 4.3: Experimental parameters and conditions

| Parameters | Conditions |
|--|---------------|
| Finishing cycle time | 60 min |
| Carbonyl iron powder (20 volume %) | 800 mesh |
| Workpiece material (Mild steel: Hardness : 427HV, 43.15HRC, 404 BHN) | Ferromagnetic |

4.3.1 Workpiece Detail

The workpiece is made up of mild steel as it is ferro-magnetic in nature. The CAD model of the workpiece is shown in Fig. 4.1. This ferro-magnetic workpiece finds its wide applications in macaroni manufacturing machine. The ultra fine surface finishing required at the outer surface of workpiece in order to reducing the frictional and wearing losses.

The workpiece is prepared on conventional lathe machine as shown in Fig. 4.2 a dovetail groove was cut on the workpiece length. This is done because the workpiece is in circular cross-sectional it is not easy to measure the surface morphology under a scanning electron microscopy (SEM). To overcome this difficulty some small keys are cut in the workpiece of dimension 10x6x3 mm. A small strip of size 10x6x3 mm was made and inserted into the dovetail groove. The shaft is finished on cylindrical grinding after the turning and the roughness was achieved after the grinding in between 620nm to 730nm.

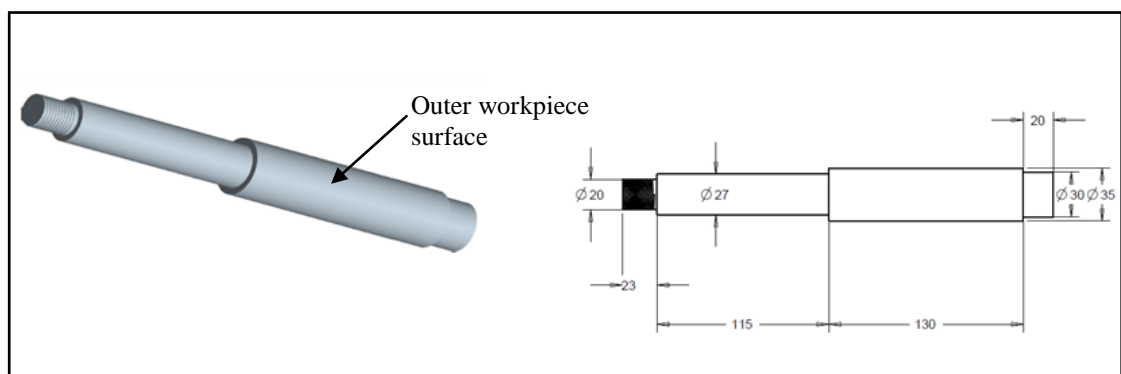


Figure 4.1: CAD model and drawing of workpiece

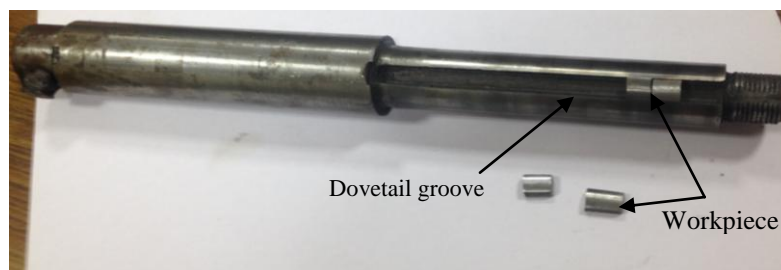


Figure 4.2: Photograph of cylindrical workpiece with dovetail groove

Table 4.4: Plan of experiments

| Std. order | Run order | Actual values | | | |
|------------|-----------|---------------|----------|-------------|----------------------|
| | | Current (A) | Gap (mm) | Speed (RPM) | Abrasive (mesh size) |
| 1 | 2 | 1.5 | 1 | 300 | 600 |
| 2 | 10 | 3.5 | 1 | 300 | 600 |
| 3 | 23 | 1.5 | 2 | 300 | 600 |
| 4 | 1 | 3.5 | 2 | 300 | 600 |
| 5 | 26 | 1.5 | 1 | 600 | 600 |
| 6 | 14 | 3.5 | 1 | 600 | 600 |
| 7 | 30 | 1.5 | 2 | 600 | 600 |
| 8 | 8 | 3.5 | 2 | 600 | 600 |
| 9 | 22 | 1.5 | 1 | 300 | 1000 |
| 10 | 6 | 3.5 | 1 | 300 | 1000 |
| 11 | 13 | 1.5 | 2 | 300 | 1000 |
| 12 | 18 | 3.5 | 2 | 300 | 1000 |
| 13 | 19 | 1.5 | 1 | 600 | 1000 |
| 14 | 24 | 3.5 | 1 | 600 | 1000 |
| 15 | 17 | 1.5 | 2 | 600 | 1000 |
| 16 | 5 | 3.5 | 2 | 600 | 1000 |
| 17 | 16 | 0.5 | 1.5 | 450 | 800 |
| 18 | 15 | 4.5 | 1.5 | 450 | 800 |
| 19 | 21 | 2.5 | 0.5 | 450 | 800 |
| 20 | 9 | 2.5 | 2.5 | 450 | 800 |
| 21 | 3 | 2.5 | 1.5 | 150 | 800 |
| 22 | 4 | 2.5 | 1.5 | 750 | 800 |
| 23 | 20 | 2.5 | 1.5 | 450 | 400 |
| 24 | 28 | 2.5 | 1.5 | 450 | 1200 |
| 25 | 12 | 2.5 | 1.5 | 450 | 800 |
| 26 | 27 | 2.5 | 1.5 | 450 | 800 |
| 27 | 29 | 2.5 | 1.5 | 450 | 800 |
| 28 | 11 | 2.5 | 1.5 | 450 | 800 |
| 29 | 25 | 2.5 | 1.5 | 450 | 800 |
| 30 | 7 | 2.5 | 1.5 | 450 | 800 |

Table 4.5: Summary of response

| Std. | Run | Factors | | | | Initial average roughness value (μm) | Final average roughness value (μm) | % Change in roughness values (% ΔRa) |
|------|-----|---------|-----|-----|------|---|---|---|
| | | I | Z | N | A | | | |
| 1 | 2 | 1.5 | 1 | 300 | 600 | 0.72 | 0.21 | 71.4286 |
| 2 | 9 | 3.5 | 1 | 300 | 600 | 0.68 | 0.17 | 74.2857 |
| 3 | 28 | 1.5 | 2 | 300 | 600 | 0.71 | 0.26 | 62.8571 |
| 4 | 30 | 3.5 | 2 | 300 | 600 | 0.65 | 0.21 | 67.1429 |
| 5 | 4 | 1.5 | 1 | 600 | 600 | 0.72 | 0.32 | 55.7143 |
| 6 | 12 | 3.5 | 1 | 600 | 600 | 0.7 | 0.28 | 60 |
| 7 | 6 | 1.5 | 2 | 600 | 600 | 0.67 | 0.36 | 45.7143 |
| 8 | 10 | 3.5 | 2 | 600 | 600 | 0.65 | 0.28 | 57.1429 |
| 9 | 19 | 1.5 | 1 | 300 | 1000 | 0.71 | 0.49 | 31.4286 |
| 10 | 15 | 3.5 | 1 | 300 | 1000 | 0.73 | 0.45 | 38.5714 |
| 11 | 21 | 1.5 | 2 | 300 | 1000 | 0.69 | 0.52 | 24.2857 |
| 12 | 1 | 3.5 | 2 | 300 | 1000 | 0.66 | 0.45 | 31.4286 |
| 13 | 20 | 1.5 | 1 | 600 | 1000 | 0.7 | 0.53 | 24.2857 |
| 14 | 23 | 3.5 | 1 | 600 | 1000 | 0.62 | 0.45 | 27.1429 |
| 15 | 8 | 1.5 | 2 | 600 | 1000 | 0.74 | 0.64 | 12.8571 |
| 16 | 27 | 3.5 | 2 | 600 | 1000 | 0.72 | 0.57 | 21.4286 |
| 17 | 22 | 0.5 | 1.5 | 450 | 800 | 0.69 | 0.44 | 35.7143 |
| 18 | 7 | 4.5 | 1.5 | 450 | 800 | 0.74 | 0.42 | 42.8571 |
| 19 | 3 | 2.5 | 0.5 | 450 | 800 | 0.7 | 0.25 | 65 |
| 20 | 18 | 2.5 | 2.5 | 450 | 800 | 0.7 | 0.35 | 50 |
| 21 | 16 | 2.5 | 1.5 | 150 | 800 | 0.73 | 0.34 | 52.8571 |
| 22 | 25 | 2.5 | 1.5 | 750 | 800 | 0.75 | 0.39 | 48.5714 |
| 23 | 26 | 2.5 | 1.5 | 450 | 400 | 0.72 | 0.36 | 50 |
| 24 | 13 | 2.5 | 1.5 | 450 | 1200 | 0.74 | 0.71 | 4.05405 |
| 25 | 29 | 2.5 | 1.5 | 450 | 800 | 0.68 | 0.43 | 37.1429 |
| 26 | 17 | 2.5 | 1.5 | 450 | 800 | 0.66 | 0.46 | 30 |
| 27 | 24 | 2.5 | 1.5 | 450 | 800 | 0.69 | 0.47 | 31.4286 |
| 28 | 5 | 2.5 | 1.5 | 450 | 800 | 0.67 | 0.43 | 35.7143 |

| | | | | | | | | |
|----|----|-----|-----|-----|-----|------|------|---------|
| 29 | 11 | 2.5 | 1.5 | 450 | 800 | 0.71 | 0.50 | 30 |
| 30 | 14 | 2.5 | 1.5 | 450 | 800 | 0.7 | 0.48 | 31.4286 |

4.4 Response Surface Regression Analysis

The responses in terms of initial roughness to final surface roughness (Ra) value and percentage change in roughness value (% Δ Ra) are presented in Table 4.5.

Percentage change in Ra value is calculated as.

$$\Delta Ra (\%) = [(Ra_i - Ra_f) / Ra_i] \times 100 \quad (4.1)$$

$\Delta Ra (\%) =$ % change in surface roughness

Ra_i= Initial roughness value

Ra_f= Final roughness value

To select the highest order polynomial the sequential model sum of squares was calculated. The model is not aliased due to some additional terms are significant. Table 4.6 shows of sequential model sum of squares show contribution of increasing complexity to the total model. The significance of adding quadratic terms to two factor interactions (2FI) and linear term is highest, as it has least P- value and high F- value suggesting its suitability. Lack of fit for test is shown in table 4.7. For the selected quadratic model, the lack of fit is insignificant.

On the basis of Tables 4.6 and 4.7, quadratic model was selected. In the initial experiments all the terms such as I, Z, N, A, IZ, IN, IA, ZN, ZA, NA, I², Z², N², A² were included in the response surface model. The ANOVA for percentage change in Ra is given in Table 4.8. The Model F-value of 22.17 implies the model is significant. There is only a 0.01% chance that an F-value this large could occur due to noise. Values of "Prob > F" less than 0.0500 indicate model terms are significant. In this case I, Z, N, A, Z², N² are significant model terms. Values greater than 0.1000 indicate the model terms are not significant. If there are many insignificant model terms (not counting those required to support hierarchy), model reduction may improve your model. The "Lack of Fit F-value" of 3.93 implies there is a 7.20%

chance that a "Lack of Fit F-value" this large could occur due to noise. Lack of fit is bad -- we want the model to fit. This relatively low probability (<10%) is troubling.

Table 4.6: Sequential model sum of squares

| Source | Sum of squares | DOF | Mean square | F-value | p- value Prob > F | Remarks |
|-----------------------------|----------------|----------|---------------|--------------|----------------------|------------------|
| Mean vs Total | 52123.56 | 1 | 52123.56 | | | |
| Linear vs Mean | 6819.31 | 4 | 1704.83 | 19.94 | < 0.0001 | |
| 2FI vs Linear | 34.18 | 6 | 5.70 | 0.051 | 0.9993 | |
| Quadratic vs 2FI | 1690.32 | 4 | 422.58 | 15.35 | < 0.0001 | Suggested |
| Cubic vs Quadratic | 365.03 | 8 | 45.63 | 6.68 | 0.0107 | Aliased |
| Residual | 47.80 | 7 | 6.83 | | | |
| Total | 61080.21 | 30 | 2036.01 | | | |

DOF: Degree of freedom, 2FI*: Two factors interaction

Table 4.7: Lack of fit tests

| Source | Sum of squares | DOF | Mean square | F-value | p- value Prob > F | Remarks |
|------------------|----------------|-----------|--------------|-------------|----------------------|------------------|
| Linear | 2090.75 | 20 | 104.54 | 11.22 | 0.0069 | |
| 2FI | 2056.56 | 14 | 146.90 | 15.76 | 0.0033 | |
| <u>Quadratic</u> | <u>366.24</u> | <u>10</u> | <u>36.62</u> | <u>3.93</u> | <u>0.0720</u> | <u>Suggested</u> |
| Cubic | 1.21 | 2 | 0.60 | 0.065 | 0.9382 | Aliased |
| Pure Error | 46.60 | 5 | 9.32 | | | |

Table 4.8: ANOVA for percentage change in Ra

| Source | Sum of squares | DOF | Mean square | F-value | p- value Prob > F | Remarks |
|----------------|----------------|-----|-------------|---------|----------------------|--------------------|
| Model | 8543.81 | 14 | 610.27 | 22.17 | < 0.0001 | significant |
| I | 164.63 | 1 | 164.63 | 5.98 | 0.0273 | |
| Z | 337.50 | 1 | 337.50 | 12.26 | 0.0032 | |
| N | 465.65 | 1 | 465.65 | 16.92 | 0.0009 | |
| A | 5851.53 | 1 | 5851.53 | 212.61 | < 0.0001 | |
| IZ | 12.76 | 1 | 12.76 | 0.46 | 0.5064 | |
| IN | 2.04 | 1 | 2.04 | 0.074 | 0.7891 | |
| IA | 0.51 | 1 | 0.51 | 0.019 | 0.8935 | |
| ZN | 0.000 | 1 | 0.000 | 0.000 | 1.0000 | |
| ZA | 0.51 | 1 | 0.51 | 0.019 | 0.8935 | |
| NA | 18.37 | 1 | 18.37 | 0.67 | 0.4268 | |
| I ² | 83.61 | 1 | 83.61 | 3.04 | 0.1018 | |
| Z ² | 1088.46 | 1 | 1088.46 | 39.55 | < 0.0001 | |
| N ² | 581.16 | 1 | 581.16 | 21.12 | 0.0004 | |
| A ² | 47.70 | 1 | 47.70 | 1.73 | 0.2078 | |
| Residual | 412.84 | 15 | 27.52 | | | not significant |
| Lack of Fit | 366.24 | 10 | 36.62 | 3.93 | 0.0720 | |

Other ANOVA parameters are given in Table 4.9. The 'predicted R^2 ' value helps to measure how good the model predicts a response value. The "Pred R-Squared" of 0.7570 is in reasonable agreement with the "Adj R-Squared" of 0.9109; i.e. the difference is less than 0.2. "Adeq Precision" measures the signal to noise ratio. A ratio greater than 4 is desirable. In the above model, this ratio of 19.864 indicates an adequate signal.

Table 4.9: Other ANOVA parameters

| | | | |
|-------------------|---------|----------------|--------|
| Std. Dev. | 5.25 | R-Squared | 0.9539 |
| Mean | 41.68 | Adj R-Squared | 0.9109 |
| C.V. % | 12.59 | Pred R-Squared | 0.7570 |
| PRESS | 2176.64 | Adeq Precision | 19.864 |
| -2 Log Likelihood | 163.79 | BIC | 214.81 |
| | | AICc | 228.08 |

S.D.: standard deviation, C.V.: Coefficient of variation, *Predicted residual sum of squares.

Table 4.10: Factor coefficients

| Factor | Coefficient Estimate | DOF | Standard error | 95% CI Low | 95% CI High | VIF |
|----------------|----------------------|-----|----------------|------------|-------------|------|
| Intercept | 32.62 | 1 | 2.14 | 28.05 | 37.18 | |
| A-I | 2.62 | 1 | 1.07 | 0.34 | 4.90 | 1.00 |
| B-Z | -3.75 | 1 | 1.07 | -6.03 | -1.47 | 1.00 |
| C-N | -4.40 | 1 | 1.07 | -6.69 | -2.12 | 1.00 |
| D-A | -15.61 | 1 | 1.07 | -17.90 | -13.33 | 1.00 |
| AB | 0.89 | 1 | 1.31 | -1.90 | 3.69 | 1.00 |
| AC | 0.36 | 1 | 1.31 | -2.44 | 3.15 | 1.00 |
| AD | 0.18 | 1 | 1.31 | -2.62 | 2.97 | 1.00 |
| BC | 0.000 | 1 | 1.31 | -2.80 | 2.80 | 1.00 |
| BD | -0.18 | 1 | 1.31 | -2.97 | 2.62 | 1.00 |
| CD | 1.07 | 1 | 1.31 | -1.72 | 3.87 | 1.00 |
| A ² | 1.75 | 1 | 1.00 | -0.39 | 3.88 | 1.05 |
| B ² | 6.30 | 1 | 1.00 | 4.16 | 8.43 | 1.05 |
| C ² | 4.60 | 1 | 1.00 | 2.47 | 6.74 | 1.05 |
| D ² | -1.32 | 1 | 1.00 | -3.45 | 0.82 | 1.05 |

DOF: Degrees of freedom, CI: Confidence interval, VIF: Variance inflation factor.

For the coefficient estimate for the factor the 95% low and high confidence interval (CI) values are the lower and upper bound of the 95% confidence interval. These values in Table 4.10 represent the range that the true coefficient should be found in 95% of the time. If this range shows 0 (one limit is positive and

the other negative) then the value of the coefficient of 0 could be true, indicating no effect of the factors. Lack of orthogonality in the design is measured by the variance inflation factor (VIF). If the value of VIF is one it shows factor is orthogonal to all other factors. If factors are too correlated together the value of VIF is greater than 10. Depending on the coefficients calculated in Table 4.10, the final equation is given as:

$$\begin{aligned} \% \Delta R_a = & 222.80295 - 10.57473 I - 86.12934 Z - 0.24801 N - 0.040947 A + 1.78571 I \\ & Z + 2.38095E-003 I N + 8.92857E-004 I A + 1.08816E-017 Z N - 1.78571E-003 Z \\ & A + 3.57143E-005 N A + 1.74590 I^2 + 25.19788 Z^2 + 2.04580E-004 N^2 - 3.29694E-005 A^2 \end{aligned} \quad (4.2)$$

For the model to be insignificant the p-value is greater than 0.05. There are as p-value greater than 0.05 indicates that the model terms are not significant. There are eight insignificant model terms (Table 4.8), to improve the model dropping insignificant terms. The ANOVA analysis after dropping the insignificant terms is presented in Tables 4.12 and 4.13. The model F-value of 61.96 implies the model is significant. Values of 'Prob > F' less than 0.05 indicates that the model terms are significant. In this case N, I, Z, N² and I² are significant model terms.

Table 4.11: ANOVA for % change in Ra after dropping the insignificant terms

| Source | Sum of squares | DOF | Mean square | F-value | p- value Prob > F | Remarks |
|----------------|----------------|-----|-------------|---------|----------------------|-----------------|
| Model | 8357.16 | 6 | 1392.86 | 53.44 | < 0.0001 | Significant |
| I | 164.63 | 1 | 164.63 | 6.32 | 0.0194 | |
| Z | 337.50 | 1 | 337.50 | 12.95 | 0.0015 | |
| N | 465.65 | 1 | 465.65 | 17.87 | 0.0003 | |
| A | 5851.53 | 1 | 5851.53 | 224.50 | < 0.0001 | |
| Z ² | 1109.72 | 1 | 1109.72 | 42.58 | < 0.0001 | |
| N ² | 588.78 | 1 | 588.78 | 22.59 | < 0.0001 | |
| Residual | 599.49 | 23 | 26.06 | | | not significant |
| Lack of Fit | 552.89 | 18 | 30.72 | 3.30 | 0.0956 | |
| Pure Error | 46.60 | 5 | 9.32 | | | |

Table 4.12: Other ANOVA parameters after model reduction

| | | | |
|-------------------|---------|----------------|--------|
| Std. Dev. | 5.11 | R-Squared | 0.9331 |
| Mean | 41.68 | Adj R-Squared | 0.9156 |
| C.V. % | 12.25 | Pred R-Squared | 0.8533 |
| PRESS | 1313.56 | Adeq Precision | 27.741 |
| -2 Log Likelihood | 174.98 | BIC | 198.79 |
| | | AICc | 194.07 |

Factor reduction after model reduction as given in table 4.13 represents the range of true coefficient.

The final equation is:

$$\% \Delta R_a = 210.58257 + 2.61905 I - 82.45294 Z - 0.21135 N - 0.078073 A + 24.98431 Z^2 + 2.02207E-004 N^2 \quad (4.3)$$

Table 4.13: Factor coefficients after model reduction

| Factor | Coefficient Estimate | DOF | Standard error | 95% CI Low | 95% CI High | VIF |
|----------------|----------------------|-----|----------------|------------|-------------|------|
| Intercept | 33.05 | 1 | 1.47 | 30.00 | 36.09 | |
| I | 2.62 | 1 | 1.04 | 0.46 | 4.77 | 1.00 |
| Z | -3.75 | 1 | 1.04 | -5.91 | -1.59 | 1.00 |
| N | -4.40 | 1 | 1.04 | -6.56 | -2.25 | 1.00 |
| A | -15.61 | 1 | 1.04 | -17.77 | -13.46 | 1.00 |
| Z ² | 6.25 | 1 | 0.96 | 4.27 | 8.23 | 1.01 |
| N ² | 4.55 | 1 | 0.96 | 2.57 | 6.53 | 1.01 |

Table 4.14: Percentage contribution of process parameter in final response of Ra

| Source | Sum of squares | % contribution |
|----------------|----------------|----------------|
| I-(Current) | 164.63 | 1.92 |
| Z-(Gap) | 337.5 | 3.94 |
| N-(Speed) | 465.65 | 5.44 |
| A-(Abrasive) | 5851.53 | 68.32 |
| Z ² | 1109.72 | 12.96 |
| N ² | 588.78 | 6.88 |
| Pure error | 46.59 | 0.54 |

4.5 Results and Discussion

Based on the results Eq.4.3 obtained after regression analysis, the results in terms of effect of magnetizing current, rotational speed of workpiece and working gap on the change in % ΔRa have been observed and computed. The effects of these variables in % change in Ra have been discussed as following.

4.5.1 Effect of Rotational Speed of Workpiece

As seen in Fig 4.3 with increase in rotation speed of the workpiece the % change in surface roughness value reduces. The effect of rotational speed on % change in surface reduction value at varying magnetizing current, 1.5mm working gap and 800 mesh size abrasives. This is because at higher rotational speed the centrifugal force increases at workpiece which is much more than the magnetic force at the tip this results in MR polishing fluid is not in stable form in the working gap during finishing. Normal magnetic force helps to impinge the abrasive particles in the workpiece and rotation speed (cutting force) is responsible for removing the material. At higher rotational speed, the centrifugal force is much higher than normal magnetic force. Due to normal magnetic force abrasive impinge in the workpiece but because of higher centrifugal force the CIP's chains not able to hold the abrasive and break before material remove from the workpiece Fig. 4.4. Therefore, for maximum the percentage reduction in the surface roughness minimum rotational speed of workpiece is required.

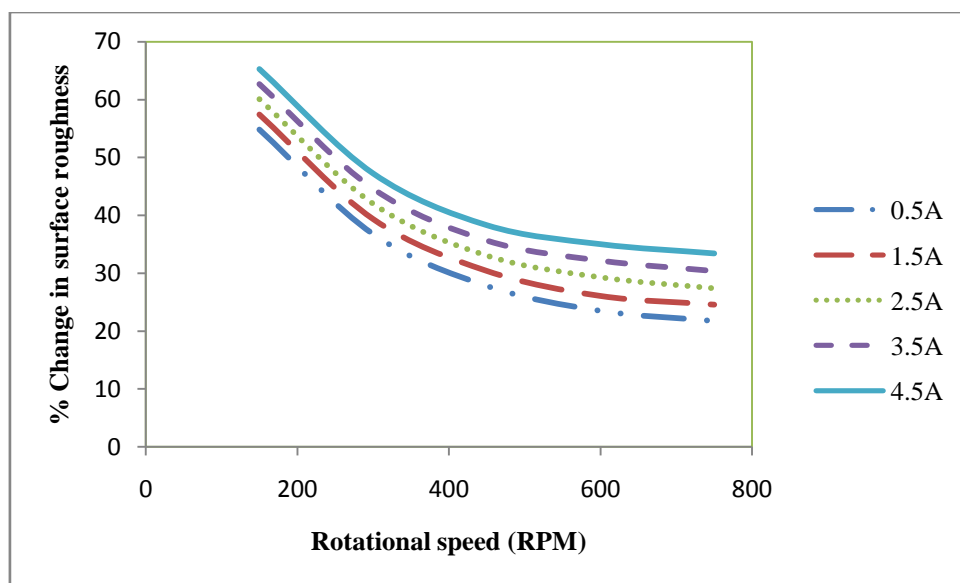


Figure 4.3: Effect of rotation speed of workpiece on percentage reduction in Ra value

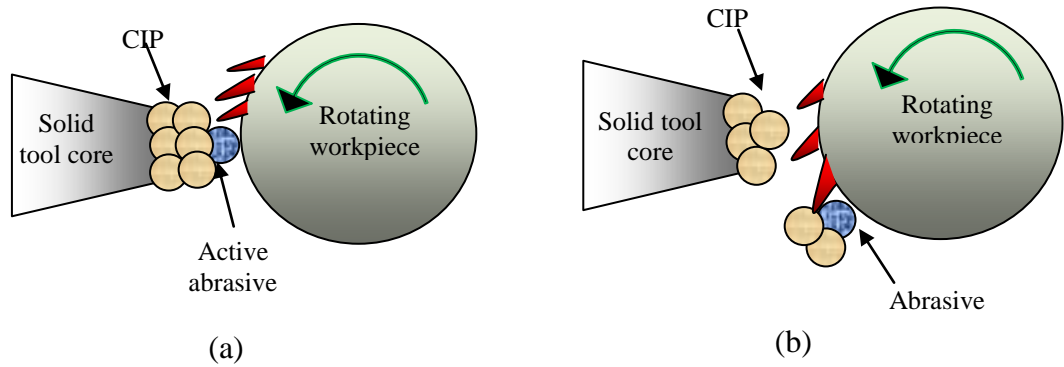


Figure 4.4: Schematic of effect of rotational speed on CIP chains (a) at low rotational speed the chains strong enough to oppose the centrifugal force and done finishing, (b) at high rotational speed the CIP chains breaks due to high centrifugal force

4.5.2 Effect of Magnetizing Current

The effect of the magnetizing current on the percentage change in surface roughness value at varying working gap, 450 rpm rotational workpiece speed and abrasive mesh size 800 is shown in Fig 4.5

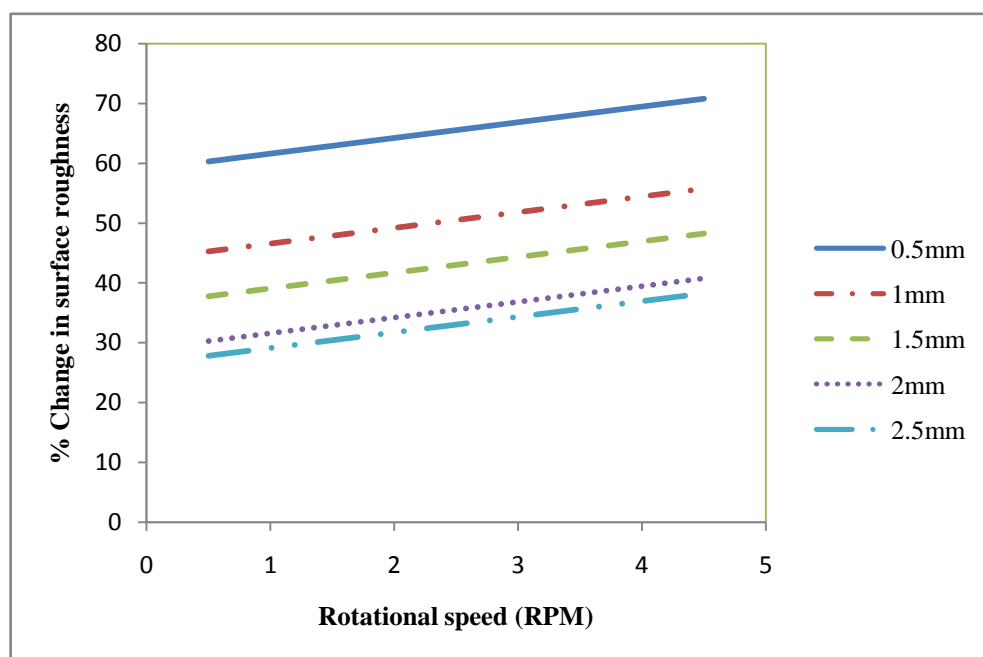


Figure 4.5: Effect of magnetizing current on percentage reduction in Ra value

The significant percentage change in roughness can be at higher magnetizing current. The magnetizing current increases the magnetic field density at

the tool tip which helps to make the strong chains of CIP's and strong chains hold the abrasives tightly which results in more percentage change in the roughness. By increasing magnetizing current increase in radial force which helps to more impingement of abrasive in the workpiece and results increase the material removal. The contour and 3D plot for the effect of rotational speed of the workpiece and working gap on the % change in R_a as shown in Fig. 4.6.

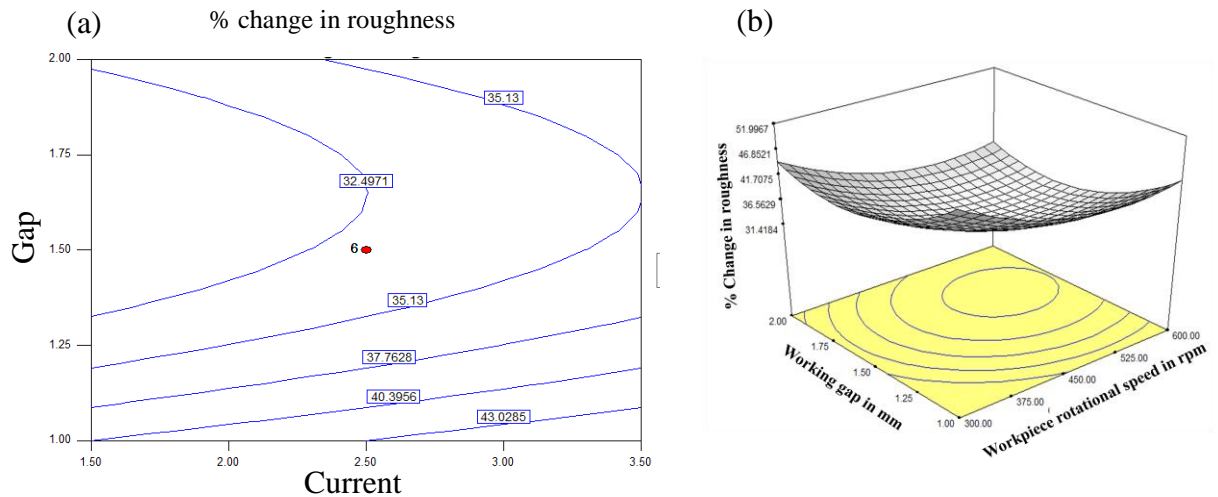


Figure 4.6 (a) Contour and (b) 3D plot of the variation of the % R_a value with working gap and workpiece rotational speed

4.5.3 Effect of Working Gap

The effect of working gap on percentage change in R_a value at different rotation speed of the workpiece with 2.5 A magnetizing current and abrasive mesh size 800 as shown in Fig. 4.7. It is observed that as the working gap between the tool and the workpiece is increase the % change in R_a value decreased. Magnetic Flux density is inversely proportional to the working gap. Therefore, when the working gap is minimizing the magnetic flux density is maximum at same current to the electromagnet coil and vice versa.

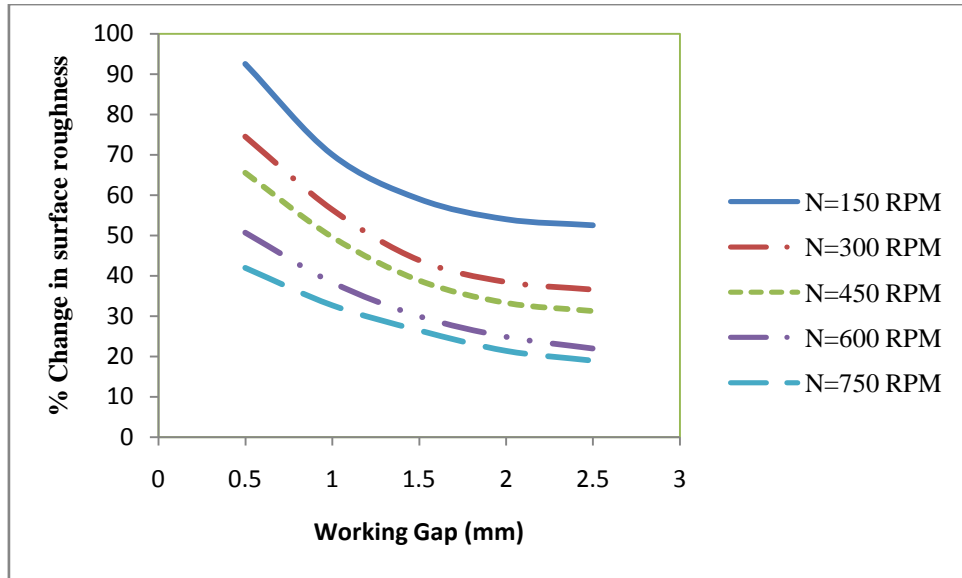


Figure 4.7: Effect of working gap on percentage reduction in Ra value

It is clear in the Fig 4.7 when working gap is reduced the percentage change in the roughness value is increased. As the working gap is less, the magnetic flux density is more at same current which results higher normal magnetic force on workpiece surface. Corresponding shear strength gets increased that may increase the percentage reduction in R_a value. Similarly, when the working gap increased at the same current the strength of the finishing spot got decreased, which may result to decrease the magnetic line of forces on the workpiece surface. At the lower magnetic flux density the CIPs particle chains are not able to hold the abrasives strongly. Corresponding results to decrease in shear strength that may further reduce the % change in the surface roughness value.

4.5.4 Effect of Abrasive Mesh Size

It is clear from the Fig 4.8 that the percentage reduction in surface roughness is increased when the abrasive mesh size is less. Because composition of MRP fluid same for all abrasive sizes so that in case of fine abrasives (800, 1000, 1200 mesh size) the numbers of abrasives particles are increased than the number of CIP's particle. CIP particles are not in sufficient numbers which hold the abrasives properly Fig. 4.9(b). Due to weak chains the abrasives not perform finishing action properly which results very less percentage reduction in surface roughness.

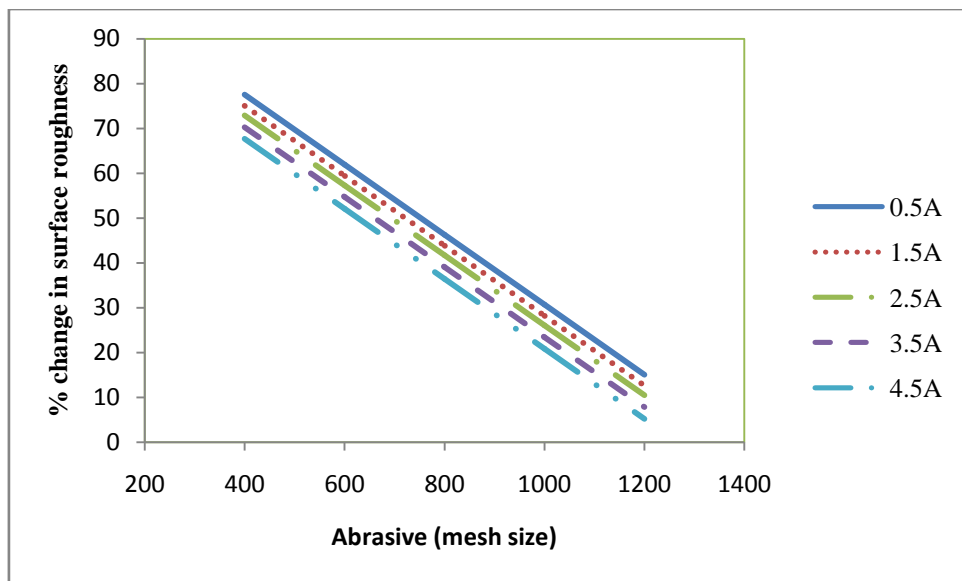


Figure 4.8: Effect of abrasive mesh size on percentage reduction in Ra value

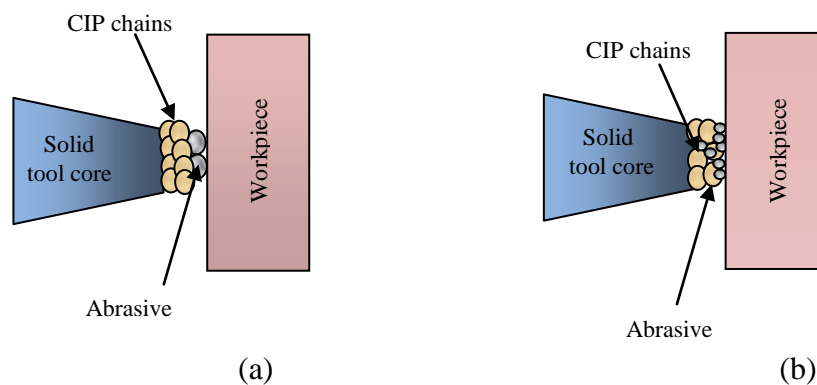


Figure 4.9: Schematic of CIP chains with abrasives (a) coarse abrasive and (b) fine abrasive

The best condition during experimentation were observed as current 3.5A, gap 1mm, rotation speed 300rpm and abrasive= 600 mesh size. The roughness obtained with these parameters 170 nm from 680 nm. The surface roughness profiles of initial and final surface and SEM images at 1000x are shown in Fig.4.10 and 4.11.

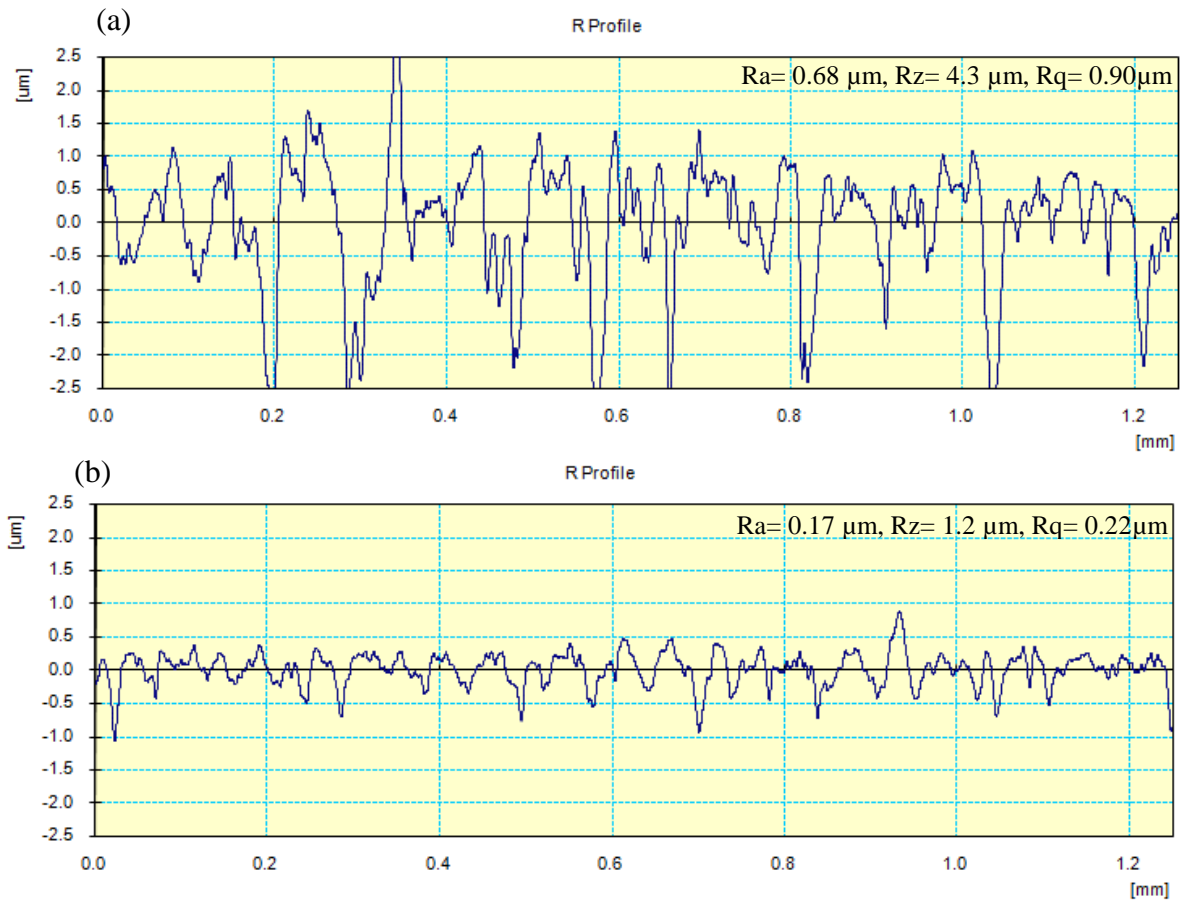


Figure 4.10: Surface roughness profile of (a) initial and (b) after finishing at current 3.5A, gap 1mm, rotation speed 300rpm and abrasive 600 mesh size for 60 minutes (Table 4.5, Exp no. 2)

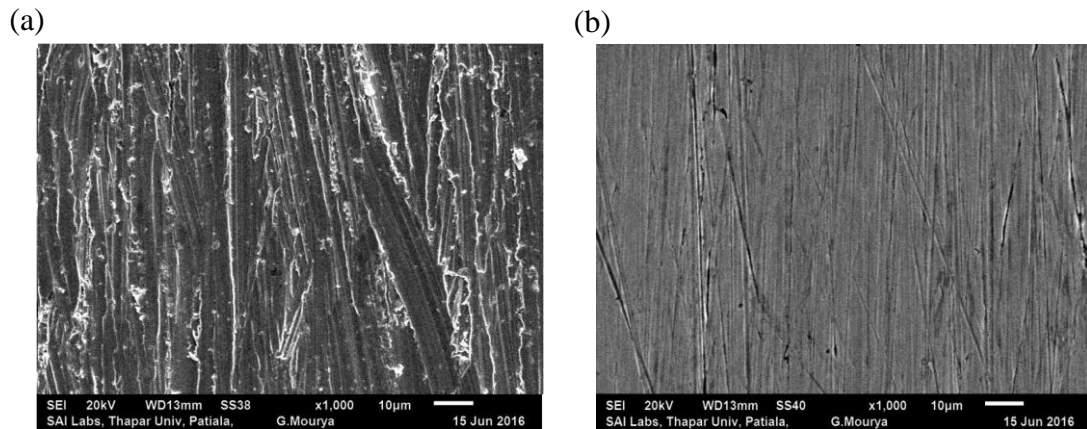


Figure 4.11: SEM micrograph at 1000x (a) initial and (b) after finishing at current 3.5A, gap 1mm, rotation speed 300rpm and abrasive 600 mesh size for 60 minutes (Table 4.5, Exp no. 2)

4.6 Confirmation Experiments for Validation of Model

Surface roughness response equation was derived from the quadratic regression fit, to verify the equation the experiments were conducted. The process variables for confirmation were selected from the contour plots. Three experiments were conducted to verify the surface roughness response equation and measured the change in roughness value. To confirm the results actual percentage change in surface roughness was compared with the predicted percentage change in roughness is listed in Table 4.15. it can be observed that the error between experimental and predicted values for $\% \Delta Ra$ lie within -6.04% to 2.43%. This confirms good reproducibility of the experimental results.

Table 4.15 Confirmation tests and their comparison with the results

| S.No | Experimental conditions | | | | Experimental ΔRa (%) | Predicted ΔRa (%) | Error (%) |
|------|-------------------------|---|-----|-----|---------------------------------|------------------------------|--------------|
| | I | Z | N | A | | | |
| 1 | 3.5 | 1 | 450 | 800 | 43.05 | 45.66 | -6.04 |
| 2 | 3.5 | 2 | 450 | 800 | 36.76 | 38.16 | -3.79 |
| 3 | 1.5 | 1 | 450 | 800 | 41.42 | 40.42 | 2.43 |

4.7 Optimization of Process

Maximum percentage change in surface roughness of the finished workpiece is required. It can be achieved by optimize the regression model.

Maximize: % ΔR_a

Subjected to

$$0.5A \leq I \leq 4.5A$$

$$0.5\text{mm} \leq D \leq 2.5\text{mm}$$

$$150 \text{ rpm} \leq N \leq 750 \text{ rpm}$$

$$400 \text{ mesh size} \leq A \leq 1200 \text{ mesh size}$$

The optimal process parameter is selected from the experimental range of the variable which lies at rotational speed of tool core 150 rpm, magnetizing current 3.5A, gap 0.5mm and abrasive mesh size 600. These parameters have been selected on the basis of their effects in percentage change in R_a after regression analysis. The data obtained from the optimum experimental conditions and their comparisons with the predicted designed for percentage change in surface roughness is listed in Table 4.16. The surface finish obtained after finishing at these conditions was 120 nm from 720 nm. The surface roughness profiles of initial and final surface are shown in Fig.4.12. SEM micrograph of initial as well as final roughness after 60 minutes of surface finishing is shown in the Fig.4.13

Table 4.16 Optimum conditions for maximizing the percentage change in surface roughness (ΔR_a)

| S.No | Optimum parameters | | | | Predicted ΔR_a (%) | Experimental ΔR_a (%) |
|------|--------------------|-----|-----|-----|----------------------------|-------------------------------|
| | I | Z | N | A | | |
| 1 | 4.5 | 0.5 | 150 | 600 | 113.39 | 83.33 |

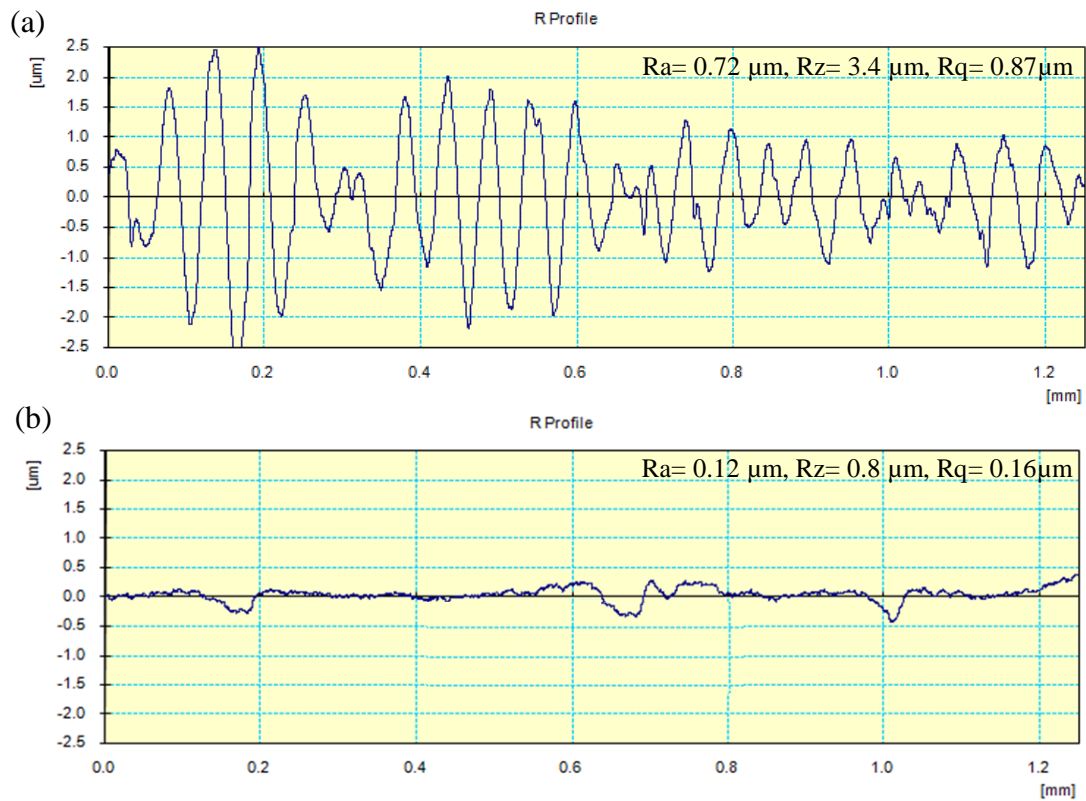


Figure 4.12: Surface roughness profile of (a) initial and (b) after finishing at optimum parameter as rotational speed of tool core 150 rpm, magnetizing current 3.5A, gap 0.5mm and abrasive mesh size 600

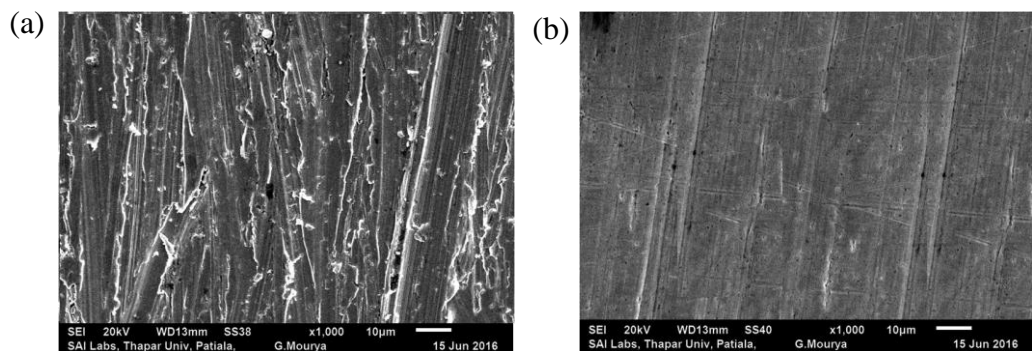


Figure 4.13: SEM micrograph at 1000x (a) initial and (b) after finishing at optimum parameter as rotational speed of tool core 150 rpm, magnetizing current 3.5A, gap 0.5mm and abrasive mesh size 600

4.8 Performance Evaluation of Turning Type Magnetorheological Process with Finishing Time

The change of surface roughness was also studied. The experiment done at the optimum parameters as listed in Table.4.16 current= 4.5A, gap= 0.5 mm, rotation speed= 150 rpm and abrasive= 600 mesh size was used. Fig.4.14 shows the effect of finishing time on surface roughness value of a workpiece measured at every 20 min during finishing. The first experiment was conducted for the finishing time of 20 min on ferromagnetic workpiece as per the experimental conditions. It has been found that surface roughness of workpiece was decreased significantly from initial values Ra= 580 nm to Ra= 80 nm.

Same type of workpiece was used to see the effect of finishing time on surface roughness. The initial surface roughness of the work piece was measured 580nm. The work piece was finished at optimum parameters and the roughness measured after every 20 minutes. The percentage change in surface roughness is show in Fig.4.14. After finishing the surface for 20 minutes using the selected parameters, a significant change in average roughness value has been seen. The Ra value changed from 580 nm to 200nm in the first 20 minutes.

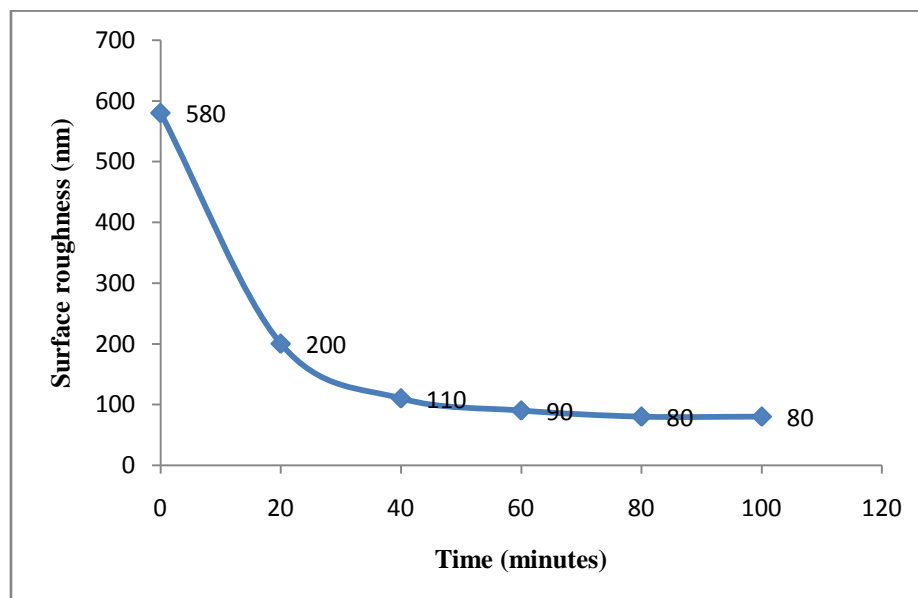


Figure 4.14: Effect of finishing time on surface roughness value

After 40 minutes, the change in the surface roughness value was not as much as compared to the previous change in roughness values. The Ra value changes from 200 nm to 110 nm. The roughness was decreased to 80 nm in next 40 minutes. In the last cycle, i.e. after 100 minutes no variation in surface roughness value was observed. The shear modulus of is more at the bottom of the peak than the top of the peak so there is no further reduction in surface roughness at same parameters. To reduce the more surface roughness parameters could be changed like composition of MRP fluid, abrasive mesh size and other experimental parameters. The surface roughness was measured before and after finishing and the roughness profile and SEM micrograph of initial as well as final roughness after 80 minutes of surface finishing is shown in the Fig.4.15 & 4.16. Before finishing, the surface image showed scratches as well as tooling marks however after the process of finishing the surface seemed very clear and free from scratches.

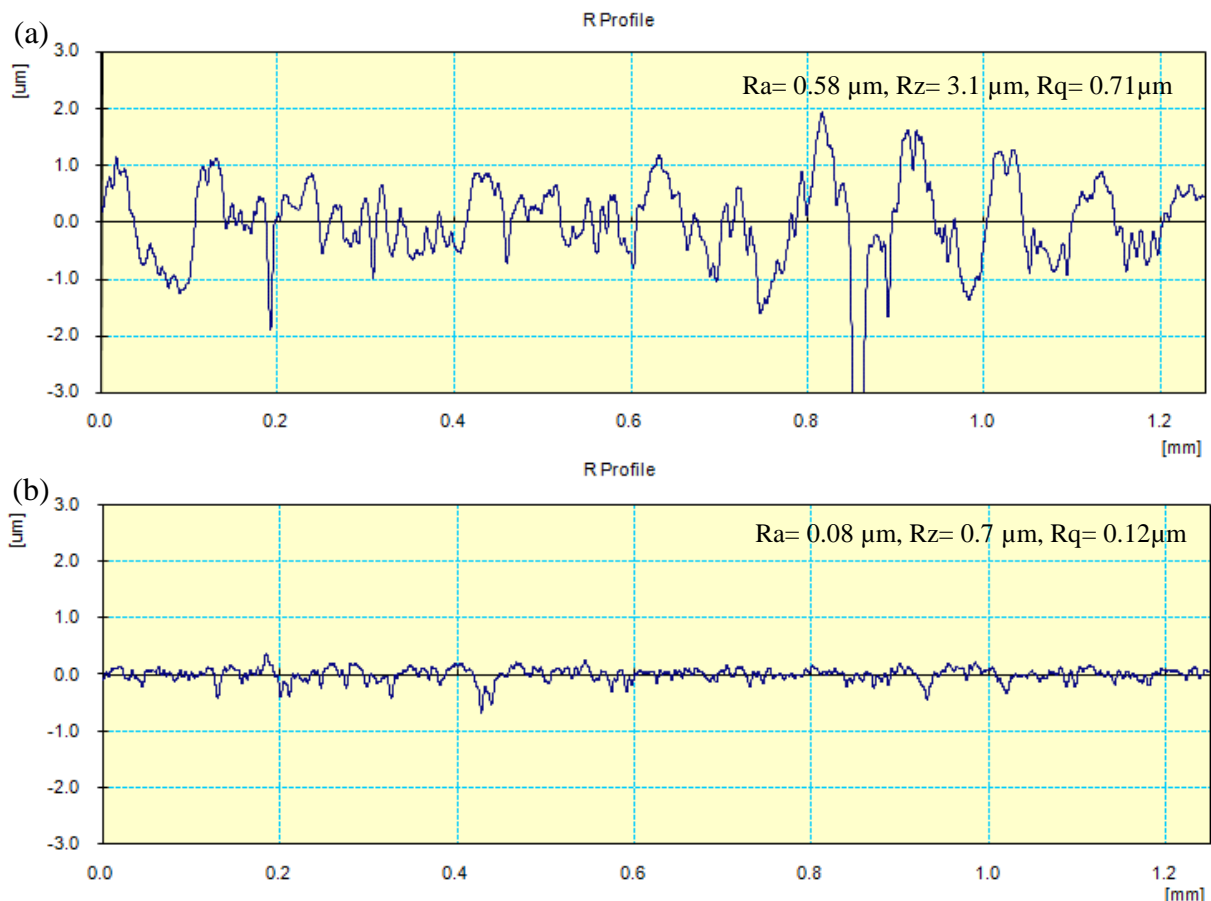


Figure 4.15: Surface roughness profiles of (a) initial and (b) after finishing at best condition current 3.5A, gap 1mm, rotation speed 300rpm and abrasive 600 mesh size

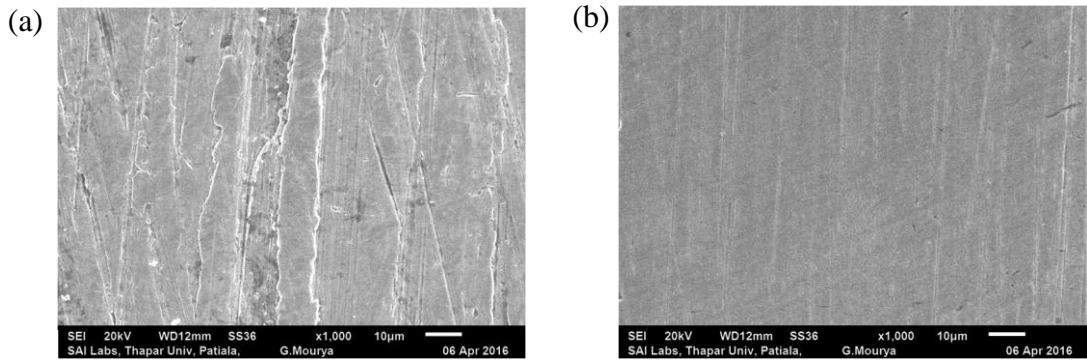


Figure 4.16: SEM micrograph at 1000x (a) initial and (b) after finishing at best condition current 3.5A, gap 1mm, rotation speed 300rpm and abrasive 600 mesh size

4.9 Conclusion

It has been seen that after experiments the parameters contributes significantly change in percentage of surface roughness value during finishing process. The following conclusions are made after experiments.

- Abrasive mesh size is the most significant parameter.
- The best surface finish value obtained on mild steel workpiece was 170 nm from initial 680 nm at the finishing condition current 3.5A, gap 1mm, workpiece rotation speed 300 rpm and abrasive 600 mesh size.
- The maximum surface reduction was achieved 80 nm from 580 nm when finishing was done with optimize parameter as current 4.5A, gap 0.5 mm, workpiece rotation 150 rpm and abrasive mesh size 600 after 80 minutes of finishing.

Chapter 5

Conclusions and Scope for Future Work

5.1 Conclusions

The turning type magnetorheological finishing tool with curve tip surface is successfully design and developed for finishing the external cylindrical workpiece surfaces. Uniform magnetic flux density is achieved on the curvature tool tip. Magnetic flux density distribution is analyzed at the tool tip using MAXWELL ANSOFT V13. This turning type MRF process is a controllable process that is controlled by controlling the direct current that affects the final finishing surface. Preliminary experiments were conducted on P20 steel permanent mould punch. The surface roughness value was reduced from 530 nm to 80 nm in 120 minutes at magnetizing current 2A, working gap 0.6 mm and rotational speed 284 rpm. Also, it has been seen after the planned experiments that the parameters (electric current, speed of rotation, working gap and abrasives) contributes in the finishing performance. The following conclusions are made after experiments.

- It is found that the abrasive mesh size is most significant factor in affecting the percentage change in the roughness (R_a) value of the mild steel workpiece.
- The best surface roughness value obtained on mild steel workpiece was 170 nm from the initial roughness (R_a) value 680 nm at finishing condition of current 3.5A, gap 1mm, rotation speed 300rpm and abrasive 600 mesh size.
- The surface roughness reduction value obtained on mild steel workpiece was 120 nm from the initial surface roughness (R_a) value 720 nm at optimum finishing conditions as rotational speed of tool core 150 rpm, magnetizing current 3.5A, gap 0.5mm and abrasive mesh size 600.
- The reduction in surface roughness from 580 nm to 80 nm and significant improvement in surface characteristics after 80 minutes of finishing, shows the ability of the present developed turning type MRF process.

5.2 Scope for the Future Work

The turning type MRF tool is attached on the conventional lathe. The problem of conventional lathe is that it cannot select a required rotational speed of chuck because it has only few predefined available speeds. Feed mechanism in conventional lathes is also attached with the rotation mechanism of chuck so you cannot give a particular feed to the tool at different speeds of chuck rotation. Due to these reasons, the experiments are not performed on designed parameters. The setup should be made fully computerized so that all machining parameters can be independently controlled and experiments performed on same parameters which are selected or planned.

At high magnetizing current the electromagnet coil gets heat up after 20-30 minutes. Due to this heat the core to tool also heat up. The core temperature should not increase more than the 55 °C - 60 °C during experimentation. If core temperature increases, temperature at the tool tip also increases, that may results to decrease the viscosity of the MRP fluid. Due to decrease in the viscosity of the MRP fluid the carbonyl iron particles are not able to hold the abrasives strongly. Therefore temperature of core should have maintained during the experimentation. Thus, cooling arrangement can be changed and made more effectively so that tool can perform continuous finishing.

References

- Bedi, T.S.; Singh, A.K. (2015) Magnetorheological methods for nanofinishing-A review, *Particulate Science and Technology*, DOI:10.1080/02726351.2015.1081657.
- Chen, M.; Liu, H.; Su, Y.; Yu, B.; Fang, Z. (2016) Design and fabrication of a novel magnetorheological finishing process for small concave surfaces using small ball-end permanent-magnet polishing head. *International Journal of Advance Manufacturing Technology*, 83:823–834.
- Harris, D.C. (2011) History of magnetorheological finishing. *Proceedings of the Window and Dome Technologies and Materials, SPIE*. DOI: 10.1117/12.882557.
- Das, M.; Jain, V.K.; Ghoshdastidar, P.S. (2008) Fluid flow analysis of magnetorheological abrasive flow finishing process. *International Journal of Machine Tools and Manufacture*, 48: 415-426.
- Gheisari, R.; Ghasemi, A.A.; Jafarkarimi, M.; Mohtaram, S. (2014) Experimental studies on the ultra precision finishing of cylindrical surfaces using magnetorheological finishing process. *Production & Manufacturing Research An Open Access Journal*, 2:1, 550-557.
- Guo, H.; Wu, Y.; Lu, D.; Fujimoto, M.; Nomura, M. (2014) Effects of pressure and shear stress on material removal rate in ultra-fine polishing of optical glass with magnetic compound fluid slurry. *Journal of Materials Processing Technology*, 214: 2759–2769
- Guo, H.; Wu, Y.; Lu, D.; Fujimoto, M.; Nomura, M. (2014) Ultrafine polishing of electroless nickel–phosphorus-plated mold with magnetic compound fluid slurry, *Materials and Manufacturing Processes*, 29:11-12, 1502-1509.
- Guo, Y.B.; Liu, C.R. (2002) Mechanical properties of hardened AISI 52100 steel in hard machining process. *Journal of Manufacturing Science and Engineering*, DOI: 10.1115/1.1413775.
- Hong, K.; Cho, Y.; Shin, B.; Cho, M.; Choi, S.; Cho, W.; Jae, J. (2012) Magnetorheological (MR) polishing of alumina-reinforced zirconia ceramics using diamond abrasives for dental application, *Materials and Manufacturing Processes*, 27:10, 1135-1138.
- Jain, V.K. (2008) Abrasive-based nano-finishing techniques. *Machining Science and Technology*, 12: 257-294.

- Jain, V.K. (2009) Magnetic field assisted abrasive based micro-/nano-finishing. *Journal of Materials Processing Technology*, 209: 6022-6038.
- Jang, K.; Kim, D.; Maeng, S.; Lee, W.; Han, J.; Seok, J.; Je, T.; Kang, S.; Min, B. (2012) Deburring microparts using a magnetorheological fluid, *International Journal of Machine Tools & Manufacture*, 53: 170–175.
- Jha, S.; Jain, V.K. (2004) Design and development of magnetorheological abrasive flow finishing process. *International Journal of Machine Tool and Manufacture*, 44(10): 1019-1029.
- Jha, S.; Jain, V.K. (2005) Nano finishing techniques. *Micro manufacturing and Nano-Technology*, 171-195.
- Jha, S.; Jain, V.K. (2006) Modelling and simulation of surface roughness in magnetorheological abrasive flow finishing process. *Wear*, 261: 856-866.
- Jiang, M.; Komanduri, R. (1998) On the finishing of Si₃N₄ balls for bearing applications. *Wear*, 215: 267-278.
- Jiao, L.; Wub, Y.; Wang, X.; Guo, H.; Liang, Z. (2013) Fundamental performance of magnetic compound fluid (MCF) wheel in ultra-fine surface finishing of optical glass. *International Journal of Machine Tools & Manufacture*, 75: 109–118.
- Komanduri, R. (1996) On material removal mechanisms in finishing of advanced ceramics and glasses. *CIRP Annals- Manufacturing Technology*, 45: 509-514.
- Kordonski, W.I.; Jacobs, S.D. (1999) Progress update in magnetorheological finishing. *International Journal of Modern Physics B*, 13: 2205-2212.
- Kordonski, W.I.; Golini, D. (1999) Fundamentals of magnetorheological fluid utilization in high precision finishing, *Journal of Intelligent Material Systems and Structures*, 10(9): 683-689.
- Kordonski, W. I.; Shorey, A.B.; Tricard, M. (2006) Magnetorheological jet finishing technology. *Transactions of ASME*, 128: 20-26.
- Mori, T.; Hirota, K.; Kawashima, Y. (2003) Clarification of magnetic abrasive finishing mechanism. *Journal of Materials Processing Technology*, 143-144: 682-686.
- Niranjan, M.S.; Jha, S. (2014) Flow behaviour of bidisperse MR polishing fluid and ball end MR finishing. *Procedia Materials Science*, 6: 798-804.
- Niranjan, M.; Jha, S.; Kotnala, R.K. (2014) Ball End magnetorheological finishing using bidisperse magnetorheological polishing fluid. *Materials and Manufacturing Processes*, 29: 487-492.

- Pandey, S.; Kant, S.; Mishra, V.; Khatri, N.; Ramagopal, S.V. (2013) Parametric Optimization of Ball End Magneto Rheological Finishing Process on EN-31. *International Journal of Recent Technology and Engineering*, 2:2, 2277-3878,
- Rhoades, L.J. (1988) Abrasive flow machining, *Manufacturing Engineering*, 1: 75-78.
- Sadiq, A.; Shunmugan, M.S. (2009) Investigation into magnetorheological abrasive honing. *International Journal of Machine Tools and Manufacture*, 49: 554-560.
- Sadiq, A.; Shunmugan, M.S. (2010) A novel method to improve finish on non-magnetic surface in magnetorheological abrasive honing process. *Tribology International*, 43: 1122-1126.
- Saraeian, P.; Mehr, H.S.; Moradi, B.; Tavakoli, H.; Alrahmani, O.K. (2016) Study of magnetic abrasive finishing for AISI321 stainless steel. *Materials and Manufacturing Processes*, DOI: 10.1080/10426914.2016.1140195.
- Saraswathamma, K.; Jha, S.; Rao, P.V. (2015) Experimental investigation into Ball end Magnetorheological Finishing of silicon. *Precision Engineering*, 42: 218–223.
- Seok, J.; Lee, S.O.; Jang, K.I.; Min, B.K.; Lee, S.J. (2009) Tribological properties of a magnetorheological (MR) fluid in a finishing process. *Tribology Transaction*, 52(4): 460-469.
- Shinmura, T.; Takazawa, K.; Hatano, E.; Aizawa, T. (1985) Study on magnetic abrasive process- process principles and finishing possibility. *Bulletin of the Japan Society of Precision Engineering*, 19(1): 54-55.
- Sidpara, A.; Das, M.; Jain, V.K. (2009) Rheological characterization of magnetorheological finishing fluid. *Materials and Manufacturing Processes*, 24(2): 1467-1478.
- Sidpara, A.; Jain, V.K. (2011) Experimental investigations into forces during magnetorheological fluid based finishing process. *International Journal of Machine Tools and Manufacture*, 51: 358-362.
- Sidpara, A.; Jain, V.K. (2011) Experimental investigations into forces during magnetorheological fluid based finishing process. *International Journal of Machine Tools and Manufacture*, 51: 358-362.
- Singh, A.K.; Jha, S.; Pandey, P.M. (2011) Design and development of nanofinishing process for 3D surfaces using ball end MR finishing tool. *International Journal of Machine Tools and Manufacture*, 51: 142-151.

- Singh, A.K.; Jha, S.; Pandey, P.M. (2012) Nanofinishing of fused silica glass using ball end magnetorheological finishing tool. *Materials and Manufacturing Processes*, 27: 1139-1144.
- Singh, A.K.; Jha, S.; Pandey, P.M. (2012) Nanofinishing of a typical 3D ferromagnetic workpiece using ball end magnetorheological finishing process. *International Journal of Machine Tools & Manufacture* 63: 21–31.
- Singh, A.K.; Jha, S.; Pandey, P.M. (2013) Mechanism of material removal in ball end magnetorheological finishing process. *Wear*, 302: 1180–1191.
- Uhlmann, E.; Doits, M.; Schmiedel, C. (2013) Development of a material model for visco-elastic abrasive medium in Abrasive Flow Machining. *Procedia CIRP*, 8: 351-356.
- Wang, A.C; Lee, S.J. (2009) Study the characteristics of magnetic finishing with gel abrasive, *International Journal of Machine Tools and Manufactures*, 49: 1063-1069.
- Wang, J.; Chen, W.; Han, F. (2015) Study on the magnetorheological finishing method for the WEDMed pierced die cavity. *International Journal of Advance Manufacturing Technology*, 76:1969–1975.
- Wang, Y.Q.; Yin, S.H.; Hunag, H.; Chen, F.J.; Deng, G.J. (2015) Magnetorheological polishing using a permanent magnetic yoke with straight air gap for ultra-smooth surface planarization, *Precision Engineering*, 40: 309–317.
- Yamaguchi, H.; Shinmura, T. (2004) Internal finishing process for alumina ceramic components by a magnetic field assisted finishing process. *Precision Engineering*, 28: 135-142.
- Yin, S.; Shinmura, T. (2004) Vertical-assisted magnetic abrasive finishing and deburring for magnesium alloy. *International Journal of Machine Tools and Manufacture*, 44: 1297-1303.